

Available online at www.sciencedirect.com**ScienceDirect**

Nuclear Physics B 910 (2016) 568–617

www.elsevier.com/locate/nuclphysb

The complete $O(\alpha_s^2)$ non-singlet heavy flavor corrections to the structure functions $g_{1,2}^{ep}(x, Q^2)$, $F_{1,2,L}^{ep}(x, Q^2)$, $F_{1,2,3}^{\nu(\bar{\nu})}(x, Q^2)$ and the associated sum rules

Johannes Blümlein ^{*}, Giulio Falcioni ¹, Abilio De Freitas*Deutsches Elektronen–Synchrotron, DESY, Platanenallee 6, D-15738 Zeuthen, Germany*

Received 18 May 2016; accepted 15 June 2016

Available online 22 June 2016

Editor: Tommy Ohlsson

Abstract

We calculate analytically the flavor non-singlet $O(\alpha_s^2)$ massive Wilson coefficients for the inclusive neutral current non-singlet structure functions $F_{1,2,L}^{ep}(x, Q^2)$ and $g_{1,2}^{ep}(x, Q^2)$ and charged current non-singlet structure functions $F_{1,2,3}^{\nu(\bar{\nu})P}(x, Q^2)$, at general virtualities Q^2 in the deep-inelastic region. Numerical results are presented. We illustrate the transition from low to large virtualities for these observables, which may be contrasted to basic assumptions made in the so-called variable flavor number scheme. We also derive the corresponding results for the Adler sum rule, the unpolarized and polarized Bjorken sum rules and the Gross–Llewellyn Smith sum rule. There are no logarithmic corrections at large scales Q^2 and the effects of the power corrections due to the heavy quark mass are of the size of the known $O(\alpha_s^4)$ corrections in the case of the sum rules. The complete charm and bottom corrections are compared to the approach using asymptotic representations in the region $Q^2 \gg m_{c,b}^2$. We also study the target mass corrections to the above sum rules.

© 2016 The Author(s). Published by Elsevier B.V. This is an open access article under the CC BY license (<http://creativecommons.org/licenses/by/4.0/>). Funded by SCOAP³.

^{*} Corresponding author.

E-mail address: johannes.bluemlein@desy.de (J. Blümlein).

¹ HiggsTools Fellow.

1. Introduction

Deep-inelastic scattering provides one of the most direct methods to measure the strong coupling constant from precision data on the scaling violations of the nucleon structure functions [1,2]. The present accuracy of these data also allows to measure the mass of the charm, cf. [3], and bottom quarks due to the heavy flavor contributions. The Wilson coefficients are known to 2-loop order in semi-analytic form [4–6] in the tagged-flavor case,² i.e. for the subset in which the hadronic final state contains at least one heavy quark, having been produced in the hard scattering process. The corresponding reduced cross section does not correspond to the notion of structure functions, since those are purely inclusive quantities and terms containing massless final states contribute as well. The heavy flavor contribution to inclusive deep-inelastic structure functions are described by five Wilson coefficients in the case of pure photon exchange [8–10]. In the asymptotic case $Q^2 \gg m^2$, where $Q^2 = -q^2$ denotes the virtuality of the exchanged gauge boson and m the mass of the heavy quark, analytic expressions for the Wilson coefficients have been calculated. A series of Mellin moments has been computed to 3-loop order in [10]. All logarithmic 3-loop corrections [11] as well as all N_F terms are known [12,13]. Four out of five Wilson coefficients contributing to the unpolarized deep inelastic structure functions have been calculated to 3-loop order for general values of Mellin N [12,14,15] in the asymptotic region $Q^2 \gg m^2$. In the flavor non-singlet case also the asymptotic 3-loop contributions to the combinations of the polarized structure functions $g_{1(2)}^{\text{NS}}$ [16] and the unpolarized charged current structure function $x F_3^{\bar{\nu}p} + x F_3^{\nu p}$ have been computed [17].

In the present paper, we calculate the complete 2-loop non-singlet heavy flavor corrections to the deep inelastic charged current structure functions $F_{1,2,3}^{\nu p}$ and the neutral current structure functions $F_{1,2}^{ep}$ and g_1^{ep} and a series of sum rules in the deep inelastic region, $Q^2 \gtrsim m_c^2$. In the asymptotic case $Q^2 \gg m^2$ the corresponding Wilson coefficients have been calculated in [11, 16–18] to $O(\alpha_s^2)$ and in [14,16,17] to $O(\alpha_s^3)$. Here the massless Wilson coefficients [19,20] to $O(\alpha_s^3)$ enter. In the tagged flavor case the corresponding corrections to $O(\alpha_s^2)$ have been calculated in [8,21] and in the asymptotic charged current case in [22].³

The associated sum rules are the Adler sum rule [23], the unpolarized Bjorken sum rule [24], the polarized Bjorken sum rule [25], and the Gross–Llewellyn Smith sum rule [26]. A central observation in the inclusive case is that there are no logarithmic corrections for the associated sum rules at large Q^2 , which are present in the tagged flavor case [27,28], however. The complete massive $O(\alpha_s^2)$ corrections to the structure functions improves the accuracy towards lower values of Q^2 . In the case of the sum rules, the corresponding contributions are found to be of the order of the known massless 4-loop corrections. We will also consider the target mass corrections to the sum rules, since they are relevant in the region of low Q^2 .

The paper is organized as follows. In Section 2 we present a general outline on the massive Wilson coefficients for the structure functions which will be considered. The $O(\alpha_s^2)$ corrections to the polarized non-singlet neutral current structure functions $g_1^{ep,\text{NS}}$ and $g_2^{ep,\text{NS}}$ are derived in detail in Section 3 as an example. In Section 4 we discuss the corrections to the neutral current structure functions $F_{1(2)}^{ep,\text{NS}}$, and in Section 5 those to the non-singlet charged current structure functions $F_{1,2,3}^{\nu(\bar{\nu})p,\text{NS}}$. Detailed numerical results are presented for all the seven non-

² For a precise implementation in Mellin space, see [7].

³ This result has been corrected in Ref. [18].

singlet structure functions for experimental use. The heavy flavor $O(\alpha_s^2)$ corrections and target mass corrections to the associated sum rules are computed in Section 6, comparing massless and massive effects and numerical results are presented for the target mass corrections. Section 7 contains the conclusions. The Appendices contain technical parts of the calculation.

2. The Wilson coefficients

We consider the heavy flavor corrections to deep-inelastic structure functions, which are inclusive observables, i.e. the hadronic final state in the corresponding differential scattering cross sections is summed over completely. Under this condition the Kinoshita–Lee–Nauenberg theorem [29,30] is valid and no infrared singularities, which have to be eventually cured by arbitrary cuts, are present [10]. As we consider deep-inelastic scattering, both the scales Q^2 and $W^2 = Q^2(1-x)/x + M^2$ have to be large enough, to probe the interior of the nucleon. Here M denotes the nucleon mass, $x = Q^2/(Sy)$ is the Bjorken variable, with $S = (p+l)^2$, and $y = p \cdot q / p \cdot l$ the inelasticity, and p and l the incoming nucleon and lepton 4-momenta. One usually demands $W^2, Q^2 \gtrsim 4 \text{ GeV}^2$. To fully avoid the region of higher twist terms, a cut $W^2 \gtrsim 12.5 \text{ GeV}^2$ [31] is necessary.

The structure functions are then given by

$$F_i(x, Q^2) = F_i^{\text{massless}}(x, Q^2) + F_i^{\text{massive}}(x, Q^2), \quad (2.1)$$

where $F_i^{\text{massless}}(x, Q^2)$ is the fully massless part of the structure function and $F_i^{\text{massive}}(x, Q^2)$ contains contributions due to a heavy quark mass m_c or m_b . Both quantities are inclusive. $F_i^{\text{massive}}(x, Q^2)$ does not correspond to the so-called tagged flavor case, demanding a heavy quark in the hadronic final state.⁴ In the asymptotic case $Q^2 \gg m^2$, the Wilson coefficients contributing to (2.1) were calculated for the non-singlet neutral current structure functions $g_{1,2}^{\text{NS}}$ and $F_{1,2}^{\text{NS}}$ and the non-singlet charged current structure function F_3^{NS} [16–18] to $O(\alpha_s^3)$ (NNLO).

The unpolarized and polarized neutral current non-singlet structure functions in the case of pure photon exchange are given by

$$F_i^{\text{NS}}(x, Q^2) = r_i \sum_{k=1}^{N_F} e_k^2 \left[C_{F_i,q}^{\text{NS}} \left(x, N_F, \frac{Q^2}{\mu^2} \right) + L_{F_i,q}^{\text{NS}} \left(x, N_F + 1, \frac{Q^2}{m^2}, \frac{m^2}{\mu^2} \right) \right] \\ \otimes \left[f_k(x, \mu^2, N_F) + f_{\bar{k}}(x, \mu^2, N_F) \right] \quad (2.2)$$

$$g_i^{\text{NS}}(x, Q^2) = \frac{1}{2} \sum_{k=1}^{N_F} e_k^2 \left[\Delta C_{g_i,q}^{\text{NS}} \left(x, N_F, \frac{Q^2}{\mu^2} \right) + \Delta L_{g_i,q}^{\text{NS}} \left(x, N_F + 1, \frac{Q^2}{m^2}, \frac{m^2}{\mu^2} \right) \right] \\ \otimes \left[\Delta f_k(x, \mu^2, N_F) + \Delta f_{\bar{k}}(x, \mu^2, N_F) \right], \quad (2.3)$$

with $i = 1, 2$. Here N_F is the number of active flavors, e_k the electric charge of the massless quarks, and $r_1 = \frac{1}{2}, r_2 = x$; $C_{i,q}^{\text{NS}}$ and $\Delta C_{i,q}^{\text{NS}}$ denote the corresponding massless Wilson coefficients and $L_{i,q}^{\text{NS}}$ and $\Delta L_{i,q}^{\text{NS}}$ the massive ones, $f_k(\bar{k})$ and $\Delta f_k(\bar{k})$ are the unpolarized (polarized)

⁴ The request to tag heavy quarks in the final state usually leads to jet-cone definitions and thus to additional unphysical logarithmic contributions. In the past the idea to rather compute tagged heavy flavor structure functions up to next-to-leading order (NLO) was motivated by experimental measurements [4,8,21,22].

quark and anti-quark distribution functions, and μ^2 is the factorization scale. Here we follow again the convention used in [9], (2.26). The notion ‘ $N_F + 1$ ’ in $(\Delta)L_q^{\text{NS}}$ means that the Wilson coefficient is calculated for N_F massless and one massive flavor.⁵

For the unpolarized charged current structure functions $F_{1,2,3}(x, Q^2)$ a second Wilson coefficient $H_{i,q}^{W^+-W^-, \text{NS}}$ contributes, which in the case of charm describes the flavor excitation

$$d \sin^2(\theta_c) + s \cos^2(\theta_c) \rightarrow c \tag{2.4}$$

in addition to or without heavy flavor pair production and possible virtual heavy quark corrections. This transition contributes already at tree level. Here θ_c denotes the Cabibbo-angle [33]. The complete corrections to $O(\alpha_s)$ have been calculated in [34,35].⁶ At $O(\alpha_s^2)$ the asymptotic heavy flavor corrections have been calculated in [18] and for $x F_3^{\nu p} + x F_3^{\bar{\nu} p}$ to $O(\alpha_s^3)$ in Ref. [17]. Beyond the terms of $O(\alpha_s)$ we will use the results in the asymptotic case for the numerical illustrations given below. Note that the latter contributions are Cabibbo suppressed

$$\propto |V_{cd}|^2 (d - \bar{d}). \tag{2.5}$$

Given the present experimental accuracy, this approximation is justified, leaving the full calculation for the future.

For the transition (2.4) the momentum fraction of the massless quarks at tree-level changes, as well known, to

$$z = x \left(1 + \frac{m^2}{Q^2} \right) \equiv \frac{x}{\tilde{\lambda}}, \tag{2.6}$$

because the corresponding Wilson coefficient is a δ -distribution. This is different at higher orders, where the Wilson coefficients are given by extended distributions, [34,35]. In the asymptotic region $Q^2 \gg m^2$ the following representations hold for the Wilson coefficients $L_{i,q}^{W^+-W^-, \text{NS}}$ and $H_{i,q}^{W^+-W^-, \text{NS}}$:

$$\begin{aligned} L_{i,q}^{W^+-W^-, \text{NS}}(N_F + 1) = & a_s^2 \left[A_{qq,Q}^{(2), \text{NS}} + \hat{C}_{i,q}^{(2), W^+-W^-, \text{NS}}(N_F) \right] + a_s^3 \left[A_{qq,Q}^{(3), \text{NS}} \right. \\ & \left. + A_{qq,Q}^{(2), \text{NS}} C_{i,q}^{(1), W^+-W^-, \text{NS}}(N_F + 1) + \hat{C}_{i,q}^{(3), W^+-W^-, \text{NS}}(N_F) \right], \end{aligned} \tag{2.7}$$

$$\begin{aligned} H_{i,q}^{W^+-W^-, \text{NS}}(N_F + 1) = & 1 + a_s C_{i,q}^{(1), W^+-W^-, \text{NS}}(N_F + 1) \\ & + a_s^2 \left[A_{qq,Q}^{(2), \text{NS}} + C_{i,q}^{(2), W^+-W^-, \text{NS}}(N_F + 1) \right] \\ & + a_s^3 \left[A_{qq,Q}^{(3), \text{NS}} + A_{qq,Q}^{(2), \text{NS}} C_{i,q}^{(1), W^+-W^-, \text{NS}}(N_F + 1) \right. \\ & \left. + C_{i,q}^{(3), W^+-W^-, \text{NS}}(N_F + 1) \right] \end{aligned} \tag{2.8}$$

⁵ From 3-loop order onward there are also genuine contributions due to two different heavy quarks [32].

⁶ See also [36] and the discussion in Ref. [35].

$$= L_{i,q}^{W^+ - W^-, \text{NS}}(N_F + 1) + C_{i,q}^{W^+ - W^-, \text{NS}}(N_F), \quad i = 1, 2, 3, \quad (2.9)$$

with $a_s(\mu^2) = \alpha_s(\mu^2)/(4\pi)$, $A_{qq,Q}^{\text{NS}}$ the massive non-singlet operator matrix element (OME) [10, 14] and $C_{F3,q}^{W^+ - W^-, \text{NS}}(N_F)$ the massless Wilson coefficient up to 3-loop order. Here we use the convention

$$\hat{f}(N_F) = f(N_F + 1) - f(N_F). \quad (2.10)$$

In the following sections we calculate the Wilson coefficients $(\Delta)L_{i,q}^{\text{NS}}$ to $O(a_s^2)$ in complete form in the deep-inelastic region. In Section 3 we present the main details of the calculation, which allows us to focus on the results in the other cases.

3. The polarized non-singlet structure functions

The polarized flavor non-singlet neutral current structure functions $g_{1,2}^{\text{NS}}$ receive massless and massive QCD corrections, where the latter contribute starting at $O(a_s^2)$. In the following we will give a detailed discussion of the heavy flavor contributions to g_1^{NS} as an example. Main aspects of the calculation are given in [Appendices A and B](#).

3.1. The structure function g_1^{NS}

To $O(a_s^2)$ the non-singlet contribution for $g_1(x, Q^2)$ reads

$$\begin{aligned} g_1^{\text{NS}}(x, Q^2) = & \left[C_{g1,q} \left(x, \frac{Q^2}{\mu^2} \right) + L_{g1,q}^{\text{NS},(2)} \left(x, \frac{Q^2}{\mu^2}, \frac{m^2}{\mu^2} \right) \right] \\ & \otimes \frac{1}{2} \left[\frac{4}{9} \Delta u_v(x, \mu^2) + \frac{1}{9} \Delta d_v(x, \mu^2) + \frac{8}{9} \Delta \bar{u}(x, \mu^2) \right. \\ & \left. + \frac{2}{9} \left[\Delta \bar{d}(x, \mu^2) + \Delta \bar{s}(x, \mu^2) \right] \right]. \end{aligned} \quad (3.1)$$

Here Δu_v and Δd_v denote the polarized valence quark densities, $\Delta \bar{u}$, $\Delta \bar{d}$ and $\Delta \bar{s}$ are the polarized sea quark distributions,⁷ \otimes denotes the Mellin convolution,

$$A(x) \otimes B(x) = \int_0^1 dx_1 \int_0^1 dx_2 \delta(x - x_1 x_2) A(x_1) B(x_2) \quad (3.2)$$

and the massless Wilson coefficient is given by

$$C_{g1,q} \left(x, \frac{Q^2}{\mu^2} \right) = \delta(1 - x) + \sum_{k=1}^2 a_s^k C_{g1,q}^{(k)} \left(x, \frac{Q^2}{\mu^2} \right), \quad (3.3)$$

with

$$C_{g1,q}^{(1)} \left(x, \frac{Q^2}{\mu^2} \right) = P_{qq}^{(0)}(x) \ln \left(\frac{Q^2}{\mu^2} \right) + c_{g1,q}^{(1)}(x) \quad (3.4)$$

⁷ For a review on polarized deep-inelastic scattering, see [37].

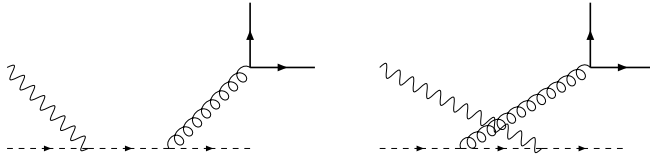


Fig. 1. The γ^*q Compton diagrams at $O(a_s^2)$. The dashed (full) lines denote massless (massive) quarks, respectively.

$$\begin{aligned}
 C_{g_1,q}^{(2)}\left(x, \frac{Q^2}{\mu^2}\right) &= \frac{1}{2} \left\{ \left[P_{qq}^{(0)} \otimes P_{qq}^{(0)} \right] (x) - \beta_0 P_{qq}^{(0)} \right\} \ln^2\left(\frac{Q^2}{\mu^2}\right) \\
 &+ \left\{ P_{qq}^{(1),\text{NS},-}(x) + \left[P_{qq}^{(0)} \otimes c_{g_1,q}^{(1)} \right] (x) - \beta_0 c_{g_1,q}^{(1)}(x) \right\} \ln\left(\frac{Q^2}{\mu^2}\right) \\
 &+ c_{g_1,q}^{(2)}(x),
 \end{aligned}
 \tag{3.5}$$

cf. e.g. [38]. Here P_{qq}^0 is the leading order splitting function

$$P_{qq}^{(0)}(x) = 2C_F \left(\frac{1+x^2}{1-x} \right)_+,
 \tag{3.6}$$

with the $+$ -prescription being defined by

$$\int_0^1 dx [f(x)]_+ g(x) = \int_0^1 dx [g(x) - g(1)] f(x).
 \tag{3.7}$$

The NLO non-singlet splitting functions $P_{qq}^{(1),\text{NS},\pm}(x)$ were calculated in [39],⁸ the quarkonic one-loop Wilson coefficient $c_{g_1,q}^{(1)}$ for the structure function g_1 [40] is given by

$$\begin{aligned}
 c_{g_1,q}^{(1)}(z) &= C_F \left[4 \left(\frac{\ln(1-z)}{1-z} \right)_+ - \left(\frac{3}{1-z} \right)_+ - 2(1+z) \ln(1-z) \right. \\
 &\left. - 2 \frac{1+z^2}{1-z} \ln(z) + 4 + 2z - \delta(1-z) [9 + 4\zeta_2] \right]
 \end{aligned}
 \tag{3.8}$$

and $c_{g_1,q}^{(2)}(z)$ has been calculated in Ref. [41]. The color factors are $C_A = N_c$, $C_F = (N_c^2 - 1)/(2N_c)$, $T_F = 1/2$ for $SU(N_c)$ and $N_c = 3$ in Quantum Chromodynamics. Here and in the following we set the factorization and renormalization scales both to μ .

The $O(a_s^2)$ Wilson coefficient $\Delta L_{g_1,q}^{\text{NS}}$ receives contributions from the Feynman diagrams shown in Figs. 1 and 2. The diagrams of the Compton process, Fig. 1, describe the real production of a heavy quark pair in the kinematic range $z \leq Q^2/(Q^2 + 4m^2)$ of the parton momentum fraction, and contain no singularities, enabling their calculation in $d = 4$ dimensions.

⁸ We use the convention $\mu^2(\partial/\partial\mu^2)$ for the scale evolution operator in the renormalization group equation.

We obtain

$$\begin{aligned}
 \Delta L_{g1,q}^{NS,(2),C} \left(z, \frac{Q^2}{m^2}, \frac{m^2}{\mu^2} \right) &= a_s^2 C_F T_F \left[\left\{ \frac{4}{3} \frac{1+z^2}{1-z} - \frac{16z}{1-z} \left(\frac{z}{\xi} \right)^2 \right\} \left\{ \left[\ln \left(\frac{1-z}{z^2} \right) \right. \right. \right. \\
 &+ \ln \left(\frac{1 + \sqrt{1 - \frac{4z}{\xi}}}{1 - \sqrt{1 - \frac{4z}{\xi}}} \right) \left. \right] \ln \left(\frac{1 + \sqrt{1 - \frac{4z}{(1-z)\xi}}}{1 - \sqrt{1 - \frac{4z}{(1-z)\xi}}} \right) \\
 &+ 2 \left[-\text{Li}_2 \left(\frac{(1-z) \left(1 + \sqrt{1 - \frac{4z}{(1-z)\xi}} \right)}{1 + \sqrt{1 - \frac{4z}{\xi}}} \right) + \text{Li}_2 \left(\frac{1 - \sqrt{1 - \frac{4z}{\xi}}}{1 + \sqrt{1 - \frac{4z}{(1-z)\xi}}} \right) \right. \\
 &+ \left. \left. \text{Li}_2 \left(\frac{1 - \sqrt{1 - \frac{4z}{(1-z)\xi}}}{1 + \sqrt{1 - \frac{4z}{\xi}}} \right) - \text{Li}_2 \left(\frac{1 + \sqrt{1 - \frac{4z}{(1-z)\xi}}}{1 + \sqrt{1 - \frac{4z}{\xi}}} \right) \right] \right\} \\
 &+ \left\{ -\frac{8}{3} + \frac{4}{1-z} + \left(\frac{z}{(1-z)\xi} \right)^2 \left(-16 + 32z - \frac{8}{1-z} \right) \right\} \\
 &\times \ln \left(\frac{1 + \sqrt{1 - \frac{4z}{(1-z)\xi}}}{1 - \sqrt{1 - \frac{4z}{(1-z)\xi}}} \right) + \left\{ \frac{64}{9} + \frac{112}{9} z - \frac{152}{9} \frac{1}{1-z} + \frac{z}{(1-z)\xi} \right. \\
 &\times \left[\frac{512}{9} - \frac{128}{3} z + \frac{848}{9} z^2 \right] + \left(\frac{z}{(1-z)\xi} \right)^2 \left[-\frac{640}{9} + \frac{1408}{9} z - \frac{2368}{9} z^2 \right. \\
 &+ \left. \left. \frac{1600}{9} z^3 \right] \right\} \frac{1}{\sqrt{1 - \frac{4z}{\xi}}} \ln \left(\frac{\sqrt{1 - \frac{4z}{\xi}} + \sqrt{1 - \frac{4z}{(1-z)\xi}}}{\sqrt{1 - \frac{4z}{\xi}} - \sqrt{1 - \frac{4z}{(1-z)\xi}}} \right) + \left\{ -\frac{188}{27} \right. \\
 &- \frac{872}{27} z + \frac{718}{27} \frac{1}{1-z} + \frac{z}{(1-z)\xi} \left[-\frac{952}{27} + \frac{1520}{27} z - \frac{800}{9} z^2 \right. \\
 &+ \left. \left. \frac{20}{27} \frac{1}{1-z} \right] \right\} \sqrt{1 - \frac{4z}{(1-z)\xi}} \left] \theta \left(\frac{\xi}{\xi + 4} - z \right), \tag{3.9}
 \end{aligned}$$

where

$$\xi = \frac{Q^2}{m^2}. \tag{3.10}$$

In [Appendix A](#) the principal steps of the calculation of (3.9) are outlined. For this contribution to $L_{g1,q}^{NS}$ we agree with the result given in [21].

The inclusive scattering cross section, however, receives also contributions from the virtual corrections shown in [Fig. 2](#).

In the Bremsstrahlung corrections (a, b) to these diagrams, the heavy flavor correction is given by the one-loop polarization function $\Pi_{QQ}(k^2 = 0)$. The polarization insertion $\Pi_{QQ}(k^2)$ also appears in the virtual correction (c). For technical reasons we decompose $\Pi_{QQ}(k^2) = \Pi_{QQ}(k^2 = 0) + [\Pi_{QQ}(k^2) - \Pi_{QQ}(k^2 = 0)]$ and combine the first term with the contributions due to (a, b). This yields the term

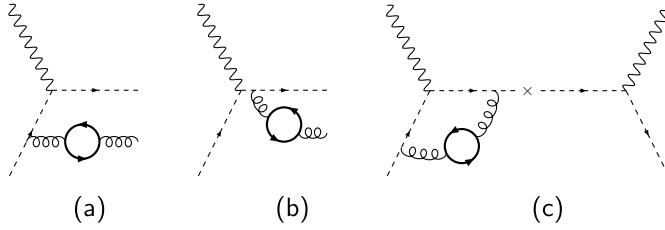


Fig. 2. The virtual $O(\alpha_s^2)$ heavy flavor corrections. (a) and (b) Bremsstrahlung amplitudes; (c) interference term of the Born amplitude and the vertex correction. The graphs of the self-energy terms contributing to (c) are not shown, but are discussed in Appendix B.

$$\Delta L_{g1,q}^{\text{NS,(2),massless}} = -a_s^2 \beta_{0,Q} \ln\left(\frac{m^2}{\mu^2}\right) \left[P_{qq}^{(0)}(z) \ln\left(\frac{Q^2}{\mu^2}\right) + c_{g1,q}^{(1)}(z) \right], \quad (3.11)$$

with $\beta_{0,Q} = -4T_F/3$. The term (3.11) corresponds to a heavy flavor contribution in the case of massless final states.

There are also self-energy insertions contributing to (c), which, however, vanish for the term (3.11) since the corresponding graphs at 1-loop vanish and $\Pi_{QQ}(k^2 = 0)$ contributes multiplicatively. For the insertion $\Pi_{QQ}(k^2 \neq 0)$ this is not the case, cf. Appendix B.

The second term $[\Pi_{QQ}(k^2) - \Pi_{QQ}(k^2 = 0)]$ is now used in the interference term calculating the form factor. The subtraction term allows to perform the calculation in $d = 4$ dimensions,

$$\begin{aligned} \Delta L_{g1,q}^{\text{NS,(2),V}}\left(\frac{Q^2}{m^2}\right) &= 2a_s^2 C_F T_F \left\{ \frac{3355}{81} - \frac{952}{9\xi} + \left(\frac{32}{\xi^2} - \frac{16}{3}\right) \zeta_3 + \left(\frac{440}{9\xi} - \frac{530}{27}\right) \ln(\xi) \right. \\ &\quad + \tilde{\lambda} \left(\frac{184}{9\xi} - \frac{76}{9}\right) \left[\text{Li}_2\left(\frac{\tilde{\lambda}+1}{\tilde{\lambda}-1}\right) - \text{Li}_2\left(\frac{\tilde{\lambda}-1}{\tilde{\lambda}+1}\right) \right] \\ &\quad \left. + \left(\frac{8}{3} - \frac{16}{\xi^2}\right) \left[\text{Li}_3\left(\frac{\tilde{\lambda}-1}{\tilde{\lambda}+1}\right) + \text{Li}_3\left(\frac{\tilde{\lambda}+1}{\tilde{\lambda}-1}\right) \right] \right\}, \quad (3.12) \end{aligned}$$

with $\tilde{\lambda} = \sqrt{1 - 4/\xi}$. Details of the calculation are presented in Appendix B.

The massive Wilson coefficient is given by

$$\begin{aligned} \Delta L_{i,q}^{\text{NS,(2)}}\left(z, \frac{Q^2}{\mu^2}, \frac{m^2}{\mu^2}\right) &= \Delta L_{i,q}^{\text{NS,(2),C}}(z, \xi) + \delta(1-z) L_{i,q}^{\text{NS,(2),V}} + \Delta L_{i,q}^{\text{NS,(2),massless}}\left(z, \frac{Q^2}{\mu^2}, \frac{m^2}{\mu^2}\right). \quad (3.13) \end{aligned}$$

In the following we will use the values

$$m_c = 1.59 \text{ GeV}, \quad m_b = 4.78 \text{ GeV} \quad (3.14)$$

at NNLO in the on-shell scheme [3,42] for all numerical illustrations, both at $O(a_s^2)$ and $O(a_s^3)$, since we consider the present results as a part of our more general NNLO project, cf. [44], and would like to compare with numerical results given at $O(a_s^3)$ in [14–17]. The transformation to the $\overline{\text{MS}}$ scheme for the heavy quark masses is well-known [45]. In fitting the heavy quark masses from data one would use the corresponding formula. For the illustration given in the following, their *equivalent* value in the on-shell scheme has been used for brevity. In the numerical results

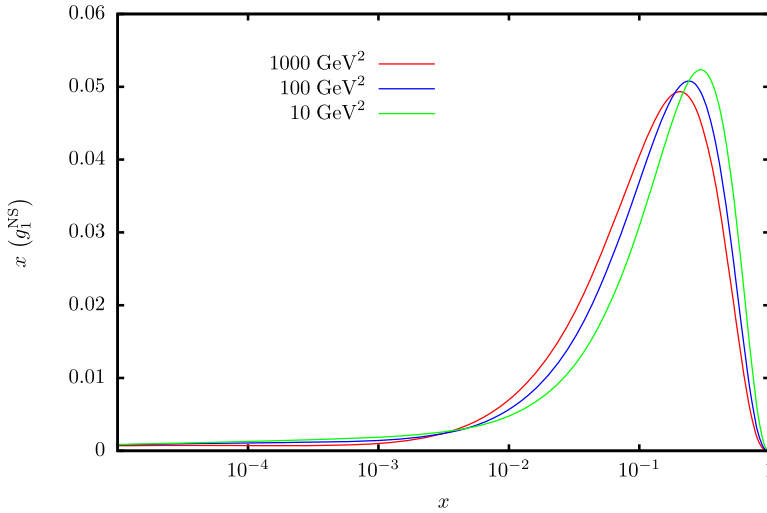


Fig. 3. The polarized structure function g_1 due to photon exchange up to $O(\alpha_s^2)$ including the charm and bottom quark corrections in the on-shell scheme with $m_c = 1.59$ GeV [3] and $m_b = 4.78$ GeV [42] using the NLO parton distribution functions [43].

given below, we choose for the factorization and renormalization scales $\mu^2 = Q^2$. In the calculation we used the codes HPLOG, CHAPLIN, HPL and HarmonicSums [46–49] at different steps, and the numerical program AIND [50].

In Fig. 3 we illustrate the massless and massive contributions to the non-singlet structure function g_1^{NS} to $O(\alpha_s^2)$ as a function of x and Q^2 using the parton distribution functions [43]. Due to the QCD evolution the peak of the function moves towards smaller values of x , keeping its valence-like profile. The contributions due to charm and bottom are illustrated in Figs. 4 and 5. Here we also compare the asymptotic expressions with the complete results, which show differences for $Q^2 \sim 10$ GeV² and become very close for $Q^2 = 100$ and 1000 GeV² for charm and at higher scales also for bottom.

The ratio of the heavy quark contributions to the complete structure function are illustrated in Fig. 6. In the range of smaller values of x the fraction amounts to $< +1.2\%$, while at larger values of x the corrections become negative amounting to -3 . The asymptotic 3-loop corrections [16] at $Q^2 = 1000$ GeV² are even larger and contribute to $O(2\%)$ at lower values of x and amount to $O(-6\%)$ at large x .

Here and in the following we often will make the observation that the asymptotic expressions tend to agree better in the region of small x even at lower values of Q^2 , where this is not expected a priori. The reason for this is that the relevant effective scale, inside the corresponding integrals, is the hadronic mass squared W^2 , rather than Q^2 itself.

3.2. The structure function g_2^{NS}

At leading twist, the structure function $g_2(x, Q^2)$ is obtained through the Wandzura–Wilczek relation

$$g_2(x, Q^2) = -g_1(x, Q^2) + \int_x^1 \frac{dy}{y} g_1(y, Q^2). \quad (3.15)$$

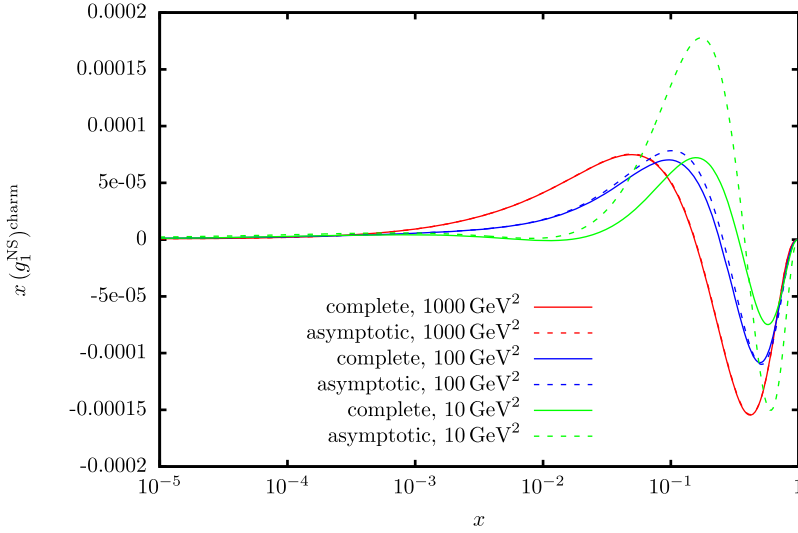


Fig. 4. The charm quark contribution to the structure function g_1 due to photon exchange up to $O(\alpha_s^2)$ as a function of x and Q^2 . The conditions are the same as in Fig. 3. Dashed lines: asymptotic representation in Q^2 for the heavy flavor corrections; full lines: complete heavy flavor contributions.

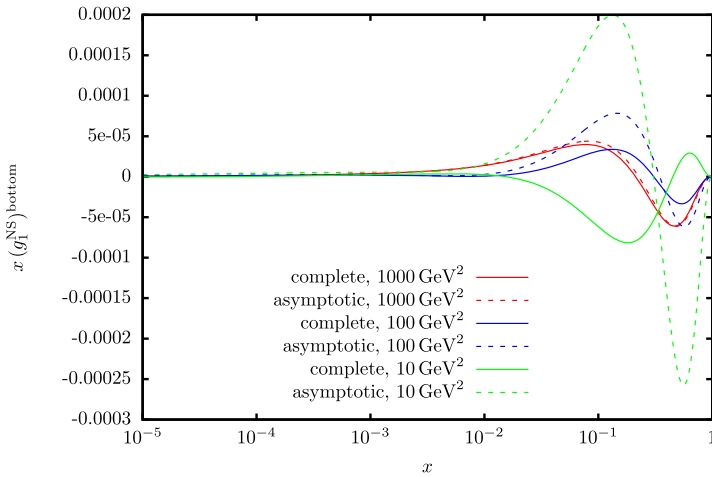


Fig. 5. The bottom quark contribution to the structure function g_1 due to photon exchange up to $O(\alpha_s^2)$ as a function of x and Q^2 . The conditions are the same as in Fig. 3. Dashed lines: asymptotic representation in Q^2 for the heavy flavor corrections; full lines: complete heavy flavor contributions.

Here $g_2(x, Q^2)$ denotes the non-singlet distribution, calculated using $g_1(x, Q^2) \equiv g_1^{\text{NS}}(x, Q^2)$, Eq. (3.1). The Wandzura–Wilczek relation has been derived for massless quarks in [51], see also [52,53], but possesses a much wider validity as has been shown in later years. It also holds for scattering off massive quarks [54] and for the target mass corrections [54,55], as well as for non-forward [56–58] and diffractive scattering [59,60] and heavy flavor production in photon–gluon fusion [61]. At leading twist the structure functions g_1 and g_2 are connected by an operator relation, cf. [56]. Representations in the covariant parton model were given in Refs. [52,61–63].

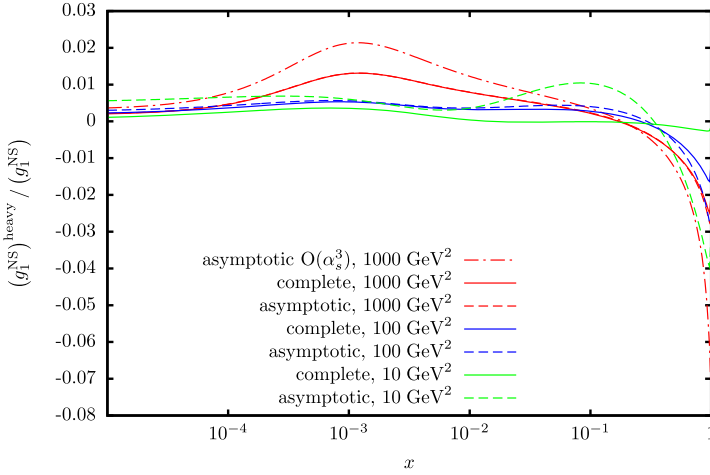


Fig. 6. The ratio of the heavy flavor non-singlet contributions to the structure function g_1 due to photon exchange to the complete structure function up to $O(\alpha_s^2)$ as a function of x and Q^2 . The conditions are the same as in Fig. 3. Dashed lines: asymptotic representation in Q^2 for the heavy flavor corrections; full lines: complete heavy flavor contributions. The dash-dotted line shows the asymptotic result at $O(\alpha_s^3)$ for $Q^2 = 1000 \text{ GeV}^2$.

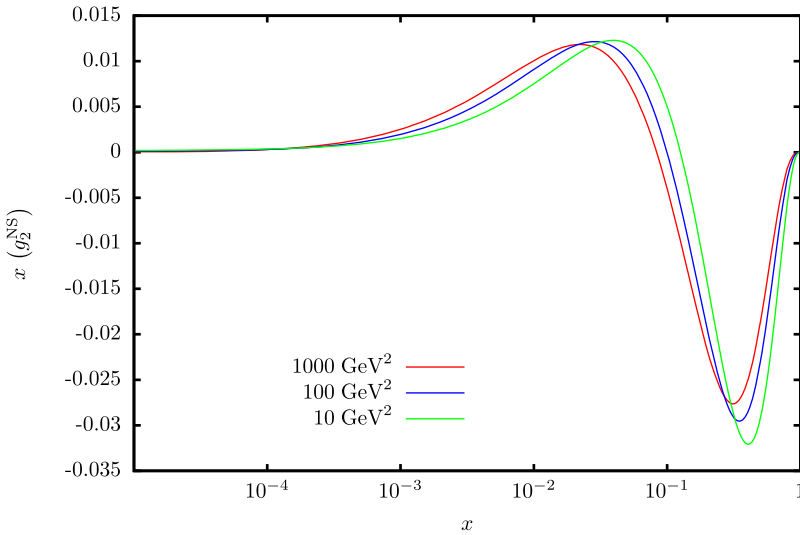


Fig. 7. The polarized structure function g_2 due to photon exchange up to $O(\alpha_s^2)$ including the charm and bottom quark corrections in the on-shell scheme with $m_c = 1.59 \text{ GeV}$ [3] and $m_b = 4.78 \text{ GeV}$ [42] using the NLO parton distribution functions [43].

In Fig. 7 we illustrate the flavor non-singlet contribution at twist 2 to the structure function $xg_2(x, Q^2)$ for pure photon exchange up to $O(\alpha_s^2)$. It takes values in the range $+0.01$ to -0.03 , with only mild scaling violations varying Q^2 from 10 GeV^2 to 1000 GeV^2 . In Figs. 8 and 9 we illustrate the heavy flavor corrections due to charm and bottom, respectively. The effect is of $O(1\%)$ in the case of charm. We also compare the exact results with those using the asymptotic representation, in which the power corrections are disregarded, cf. [16]. The effect is clearly visible at lower scales, and fully disappears at $Q^2 \sim 100 \text{ GeV}^2$ in the case of charm.

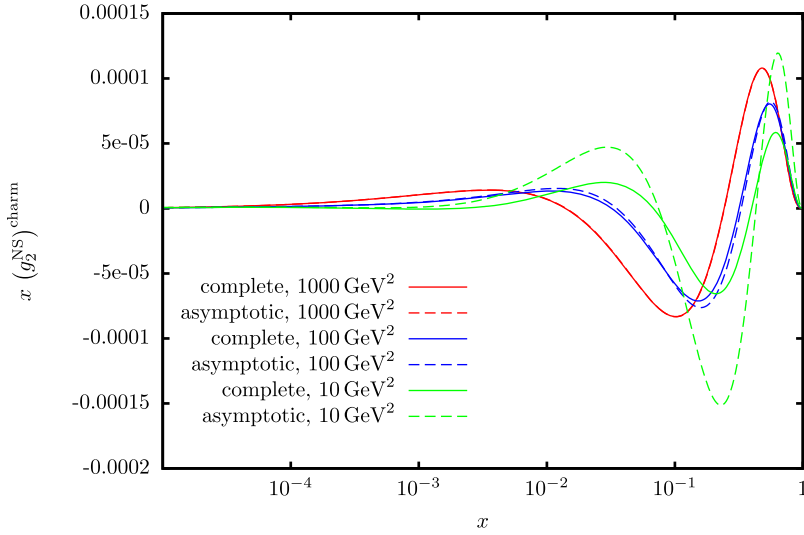


Fig. 8. The charm contribution to the structure function g_2 due to photon exchange up to $O(\alpha_s^2)$ as a function of x and Q^2 . The conditions are the same as in Fig. 7. Dashed lines: asymptotic representation in Q^2 for the heavy flavor corrections; full lines: complete heavy flavor contributions.

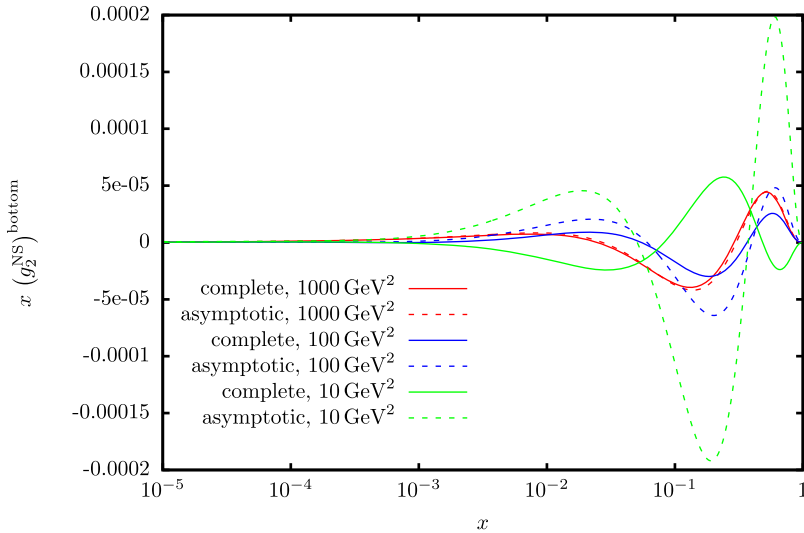


Fig. 9. The bottom contribution to the structure function g_2 due to photon exchange up to $O(\alpha_s^2)$ as a function of x and Q^2 . The conditions are the same as in Fig. 7. Dashed lines: asymptotic representation in Q^2 for the heavy flavor corrections; full lines: complete heavy flavor contributions.

In Fig. 10 we illustrate the combined heavy flavor effect and also show the asymptotic 3-loop corrections, which turn out to be larger than the exact corrections.

The structure of the Wandzura–Wilczek relation implies that the associated sum rule for the first moment yields zero. However, this is not a prediction which derives from the light-cone

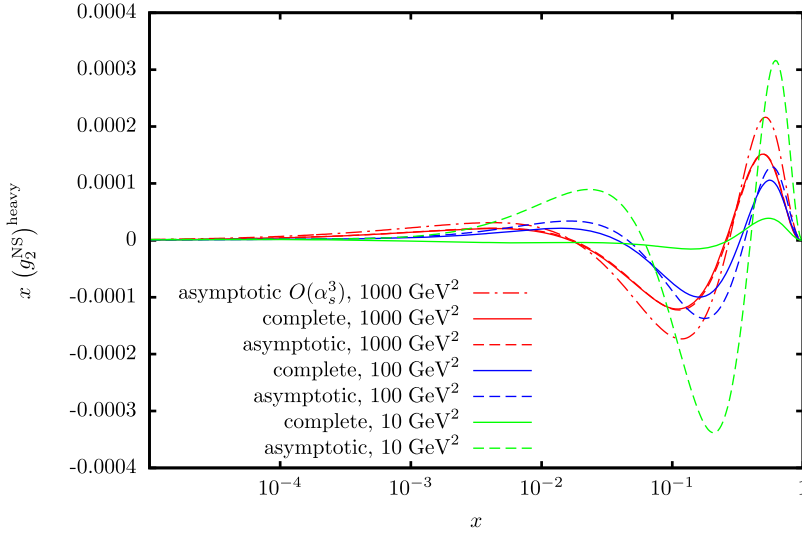


Fig. 10. The complete heavy flavor contributions to the non-singlet structure function g_2 due to photon exchange up to $O(\alpha_s^2)$ as a function of x and Q^2 . Full lines: $O(\alpha_s^2)$ contributions; dashed lines asymptotic $O(\alpha_s^2)$ contributions. The dash-dotted line for $Q^2 = 1000 \text{ GeV}^2$ corresponds to all contributions including also the asymptotic $O(\alpha_s^3)$ term. The conditions are the same as in Fig. 7.

expansion [53], since the corresponding moment does not contribute to it as a term. Rather the Wandzura–Wilczek relation, as an analytic continuation, is compatible with the result, which is also called (flavor non-singlet) Burkhardt–Cottingham sum rule [64]. It results from the fact that the imaginary part of $g_2(\bar{q}^2, q_0)$ obeys a superconvergence relation. Unlike a series of other sum rules, it cannot be expressed as an expectation value of (axial)vector operators [65].

4. The unpolarized non-singlet structure functions $F_{1,2}^{\text{NS}}$

In the case of pure photon exchange, the unpolarized neutral current scattering cross section is parameterized by two deep-inelastic structure functions $F_{1,2}(x, Q^2)$ which obey

$$2xF_1(x, Q^2) = F_2(x, Q^2) - F_L(x, Q^2), \tag{4.1}$$

in the absence of target mass corrections [66]. Here $F_L(x, Q^2)$ denotes the longitudinal structure function. In the following we will refer to the structure functions F_2 and F_L . The calculation proceeds in a similar way to that outlined in Section 3.

4.1. F_L^{NS}

In the case of the structure function F_L , the Compton contribution is given by

$$\begin{aligned} L_{F_L,q}^{\text{NS,(2),C}} \left(z, \frac{Q^2}{m^2}, \frac{m^2}{\mu^2} \right) \\ = a_s^2 C_F T_F \left\{ 96 \frac{z^3}{\xi^2} \left[\ln \left(\frac{1 + \sqrt{1 - \frac{4z}{(1-z)\xi}}}{1 - \sqrt{1 - \frac{4z}{(1-z)\xi}}} \right) \ln \left(\frac{1 + \sqrt{1 - \frac{4z}{\xi}}}{1 - \sqrt{1 - \frac{4z}{\xi}}} \right) \right] \right\} \end{aligned}$$

$$\begin{aligned}
 &+ 2 \left[-\text{Li}_2 \left(\frac{(1-z) \left(1 + \sqrt{1 - \frac{4z}{(1-z)\xi}} \right)}{1 + \sqrt{1 - \frac{4z}{\xi}}} \right) + \text{Li}_2 \left(\frac{1 - \sqrt{1 - \frac{4z}{\xi}}}{1 + \sqrt{1 - \frac{4z}{(1-z)\xi}}} \right) \right. \\
 &+ \left. \text{Li}_2 \left(\frac{1 - \sqrt{1 - \frac{4z}{(1-z)\xi}}}{1 + \sqrt{1 - \frac{4z}{\xi}}} \right) - \text{Li}_2 \left(\frac{1 + \sqrt{1 - \frac{4z}{(1-z)\xi}}}{1 + \sqrt{1 - \frac{4z}{\xi}}} \right) \right] \\
 &- \frac{16}{3\xi} (22z^2 - z\xi) \sqrt{1 - \frac{4z}{\xi}} \ln \left(\frac{\sqrt{1 - \frac{4z}{\xi}} + \sqrt{1 - \frac{4z}{(1-z)\xi}}}{\sqrt{1 - \frac{4z}{\xi}} - \sqrt{1 - \frac{4z}{(1-z)\xi}}} \right) \\
 &- \frac{8}{9(1-z)\xi} \sqrt{1 - \frac{4z}{(1-z)\xi}} \left[60z - 478z^2 + 372z^3 \right. \\
 &\left. - \xi(6 - 31z + 25z^2) \right] + \ln \left(\frac{1 + \sqrt{1 - \frac{4z}{(1-z)\xi}}}{1 - \sqrt{1 - \frac{4z}{(1-z)\xi}}} \right) \\
 &\times \left[\frac{32(6z^2 - 9z + 2)z^2}{(1-z)^2\xi^2} + 96 \frac{z^3}{\xi^2} \ln \left(\frac{1-z}{z^2} \right) \right] \theta \left(\frac{\xi}{\xi + 4} - z \right) \tag{4.2}
 \end{aligned}$$

and we confirm the result given in [8]. The virtual contribution vanishes and the contribution corresponding to massless final states reads

$$L_{F_L,q}^{\text{NS,(2),massless}} \left(z, \frac{Q^2}{\mu^2}, \frac{m^2}{\mu^2} \right) = -a_s^2 \beta_0 \cdot Q \ln \left(\frac{m^2}{\mu^2} \right) c_{F_L,q}^{(1)}(z), \tag{4.3}$$

with [67]

$$c_{F_L,q}^{(1)}(z) = 4C_{FZ}. \tag{4.4}$$

Expanding $L_{L,q}^{\text{NS,(2)}}$ for large values of ξ leads to $\hat{C}_{F_L,q}^{(2)}$, the corresponding massless 2-loop Wilson coefficient [68,69], as predicted by renormalization in Refs. [10,11] with no logarithmic term $\sim \ln(\xi)$ left, unlike the case where we take just the term $L_{q,L}^{\text{NS,(2),C}}$ into account, cf. [8,70], where [38]

$$\hat{C}_{F_L,q}^{\text{NS,(2)}}(z) = -\beta_{0,Q} c_{L,q}^{(1)} \ln \left(\frac{Q^2}{\mu^2} \right) + \hat{c}_{F_L,q}^{\text{NS,(2)}}(z), \tag{4.5}$$

and

$$\hat{c}_{F_L,q}^{\text{NS,(2)}}(z) = C_F T_F \left\{ \frac{16}{3} - \frac{200}{9}z - \frac{16}{3}z [2 \ln(z) - \ln(1-z)] \right\}. \tag{4.6}$$

The non-singlet structure function for F_L reads

$$\begin{aligned}
 F_L^{\text{NS}}(x, Q^2) &= x \left[C_{F_L,q} \left(x, \frac{Q^2}{\mu^2} \right) + L_{F_L,q}^{\text{NS,(2)}} \left(x, \frac{Q^2}{\mu^2}, \frac{m^2}{\mu^2} \right) \right] \\
 &\otimes \left[\frac{4}{9} u_v(x, \mu^2) + \frac{1}{9} d_v(x, \mu^2) + \frac{8}{9} \bar{u}(x, \mu^2) + \frac{2}{9} [\bar{d}(x, \mu^2) + \bar{s}(x, \mu^2)] \right], \tag{4.7}
 \end{aligned}$$

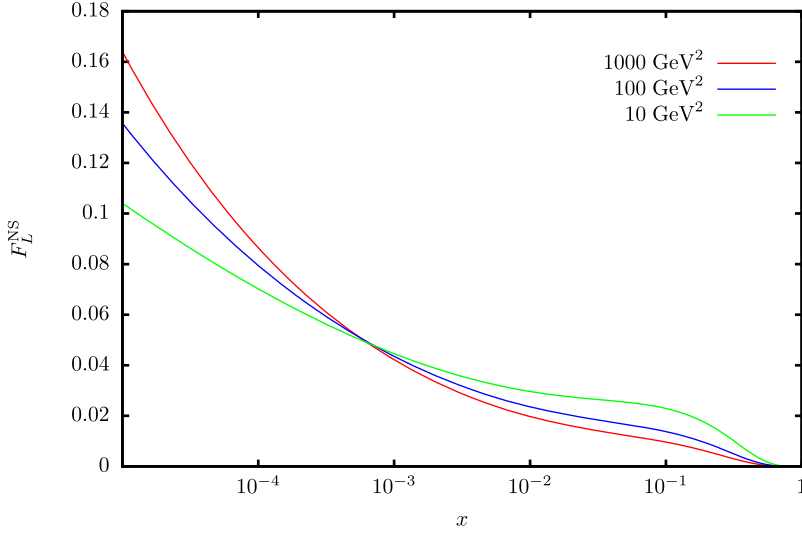


Fig. 11. The structure function F_L due to photon exchange up to $O(\alpha_s^2)$ including the charm and bottom quark corrections in the on-shell scheme with $m_c = 1.59$ GeV [3] and $m_b = 4.78$ GeV [42] using the NNLO parton distribution functions [71].

where u_v and d_v are the unpolarized valence quark densities and \bar{u} and \bar{d} the sea quark densities, and the massless Wilson coefficient is given by

$$C_{F_L,q} \left(x, \frac{Q^2}{\mu^2} \right) = \sum_{k=1}^2 a_s^k C_{F_L,q}^{(k)} \left(x, \frac{Q^2}{\mu^2} \right), \quad (4.8)$$

with [38]

$$C_{F_L,q}^{(1)} \left(x, \frac{Q^2}{\mu^2} \right) = c_{F_L,q}^{(1)}(x) \quad (4.9)$$

$$C_{F_L,q}^{(2)} \left(x, \frac{Q^2}{\mu^2} \right) = \left\{ \left[P_{qq}^{(0)} \otimes c_{F_L,q}^{(1)} \right] (x) - \beta_0 c_{F_L,q}^{(1)}(x) \right\} \ln \left(\frac{Q^2}{\mu^2} \right) + c_{F_L,q}^{(2)}(x). \quad (4.10)$$

In Fig. 11 we show the $O(\alpha_s^2)$ corrections to the non-singlet structure function F_L^{NS} , including the complete charm and bottom quark corrections. During evolution this structure function grows towards small values of x . The absolute charm and bottom quark contributions are illustrated in Figs. 12, 13. In the present case, the corrections in the asymptotic limit are sufficiently close to the complete corrections only for $Q^2 \gtrsim 1000$ GeV² in the case of charm. It is well known that for F_L the asymptotic representation holds at very high scales only, which also applies to the non-singlet case. For the charm quark corrections the asymptotic representation holds at $Q^2 \sim 1000$ GeV². Below there are significant differences. The situation is correspondingly worse for the bottom quark corrections shown in Fig. 13. In general the asymptotic corrections give larger negative corrections than found in the complete calculation. The relative heavy flavor corrections for F_L^{NS} are shown in Fig. 14. They behave nearly constant in the small x region, amounting to -0.3 to -4% in the region $Q^2 = 10$ to 1000 GeV², with larger asymptotic corrections.

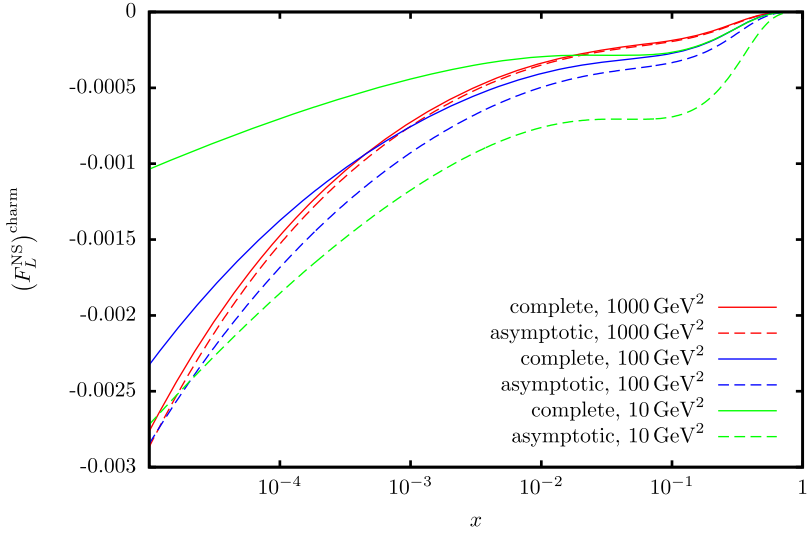


Fig. 12. The charm quark contribution to the structure function F_L due to photon exchange up to $O(\alpha_s^2)$ as a function of x and Q^2 . The conditions are the same as in Fig. 11. Dashed lines: asymptotic representation in Q^2 for the heavy flavor corrections; full lines: complete heavy flavor contributions.

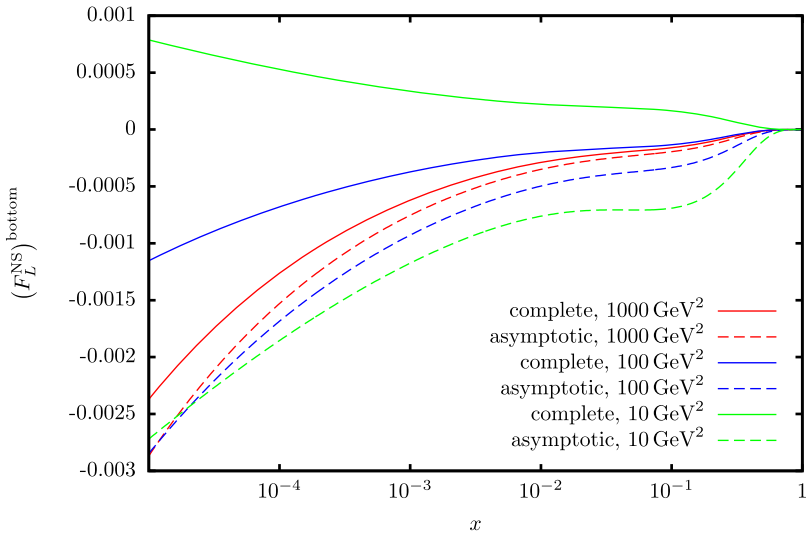


Fig. 13. The bottom quark contribution to the structure function F_L due to photon exchange up to $O(\alpha_s^2)$ as a function of x and Q^2 . The conditions are the same as in Fig. 11. Dashed lines: asymptotic representation in Q^2 for the heavy flavor corrections; full lines: complete heavy flavor contributions.

4.2. F_2^{NS}

For the structure function F_2 , we obtain the following Compton contribution

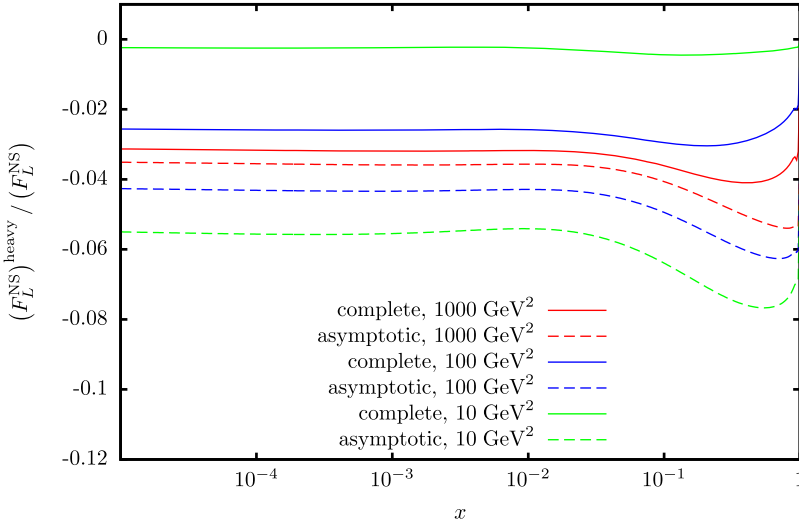


Fig. 14. The ratio of the heavy flavor contributions to the structure function F_L due to photon exchange to the complete structure function up to $O(\alpha_s^2)$ as a function of x and Q^2 . The conditions are the same as in Fig. 11. Dashed lines: asymptotic representation in Q^2 for the heavy flavor corrections; full lines: complete heavy flavor contributions.

$$\begin{aligned}
 &L_{F_2,q}^{NS,(2),C} \left(z, \frac{Q^2}{m^2}, \frac{m^2}{\mu^2} \right) \\
 &= a_s^2 C_F T_F \left\{ \left[-\frac{16z^2}{\xi^2(1-z)} (1-9z+9z^2) + \frac{4}{3} \frac{1+z^2}{1-z} \right] \right. \\
 &\quad \times \left[\left[\ln \left(\frac{1 + \sqrt{1 - \frac{4z}{\xi}}}{1 - \sqrt{1 - \frac{4z}{\xi}}} \right) + \ln \left(\frac{1-z}{z^2} \right) \right] \ln \left(\frac{1 + \sqrt{1 - \frac{4z}{(1-z)\xi}}}{1 - \sqrt{1 - \frac{4z}{(1-z)\xi}}} \right) \right. \\
 &\quad \left. \left. + 2 \left[-\text{Li}_2 \left(\frac{(1-z) \left(1 + \sqrt{1 - \frac{4z}{(1-z)\xi}} \right)}{1 + \sqrt{1 - \frac{4z}{\xi}}} \right) + \text{Li}_2 \left(\frac{1 - \sqrt{1 - \frac{4z}{\xi}}}{1 + \sqrt{1 - \frac{4z}{(1-z)\xi}}} \right) \right. \right. \right. \\
 &\quad \left. \left. \left. + \text{Li}_2 \left(\frac{1 - \sqrt{1 - \frac{4z}{(1-z)\xi}}}{1 + \sqrt{1 - \frac{4z}{\xi}}} \right) - \text{Li}_2 \left(\frac{1 + \sqrt{1 - \frac{4z}{(1-z)\xi}}}{1 + \sqrt{1 - \frac{4z}{\xi}}} \right) \right] \right] \right. \\
 &\quad \left. + \frac{8}{9(1-z)\xi} \left[26z - 168z^2 + 188z^3 - (8 - 6z + 17z^2)\xi \right] \sqrt{1 - \frac{4z}{\xi}} \right. \\
 &\quad \left. \times \ln \left(\frac{\sqrt{1 - \frac{4z}{\xi}} + \sqrt{1 - \frac{4z}{(1-z)\xi}}}{\sqrt{1 - \frac{4z}{\xi}} - \sqrt{1 - \frac{4z}{(1-z)\xi}}} \right) + \frac{2}{27(1-z)^2\xi} \sqrt{1 - \frac{4z}{(1-z)\xi}} \right. \\
 &\quad \left. \times \left[-1702z + 9516z^2 - 14260z^3 + 6456z^4 \right] \right\}
 \end{aligned}$$

$$\begin{aligned}
 & + (223 - 709z + 1108z^2 - 622z^3)\xi \Big] \\
 & - \frac{4}{3(1-z)^3\xi^2} \left[6z^2(-15 + 70z - 90z^2 + 36z^3) - \xi^2(1 - 3z^2 + 2z^3) \right] \\
 & \times \ln \left(\frac{1 + \sqrt{1 - \frac{4z}{(1-z)\xi}}}{1 - \sqrt{1 - \frac{4z}{(1-z)\xi}}} \right) \Big\} \theta \left(\frac{\xi}{\xi + 4} - z \right). \tag{4.11}
 \end{aligned}$$

This expression agrees with a result given in [8]. The virtual correction is the same as in the case of the structure function g_1^{NS} , Eq. (3.12), and the contribution with massless final states is given by:

$$\begin{aligned}
 & L_{F_{2,q}}^{\text{NS},(2),\text{massless}} \left(z, \frac{Q^2}{\mu^2}, \frac{m^2}{\mu^2} \right) \\
 & = -a_s^2 \beta_{0,Q} \ln \left(\frac{m^2}{\mu^2} \right) \left[P_{qq}^{(0)}(z) \ln \left(\frac{Q^2}{\mu^2} \right) + c_{F_{2,q}}^{(1)}(z) \right], \tag{4.12}
 \end{aligned}$$

with [72]

$$\begin{aligned}
 & c_{F_{2,q}}^{(1)}(z) = C_F \left\{ 4 \left(\frac{\ln(1-z)}{1-z} \right)_+ - \left(\frac{3}{(1-x)} \right)_+ + 6 + 4z - 2(1+z) \ln(1-z) \right. \\
 & \quad \left. - 2 \left(\frac{1+z^2}{1-z} \right) \ln(z) - (9 + 4\zeta_2) \delta(1-z) \right\}. \tag{4.13}
 \end{aligned}$$

Up to $O(a_s^2)$ the non-singlet structure function $F_2(x, Q^2)$ reads

$$\begin{aligned}
 & F_2^{\text{NS}}(x, Q^2) = x \left\{ \left[C_{F_{2,q}} \left(x, \frac{Q^2}{\mu^2} \right) + L_{F_{2,q}}^{\text{NS},(2)} \left(x, \frac{Q^2}{\mu^2}, \frac{m^2}{\mu^2} \right) \right] \right. \\
 & \quad \left. \otimes \left[\frac{4}{9} u_v(x, \mu^2) + \frac{1}{9} d_v(x, \mu^2) + \frac{8}{9} \bar{u}(x, \mu^2) + \frac{2}{9} [\bar{d}(x, \mu^2) + \bar{s}(x, \mu^2)] \right] \right\}, \tag{4.14}
 \end{aligned}$$

and the massless Wilson coefficient is given by

$$C_{F_{2,q}} \left(x, \frac{Q^2}{\mu^2} \right) = \delta(1-x) + \sum_{k=1}^2 a_s^k C_{F_{2,q}}^{(k)} \left(x, \frac{Q^2}{\mu^2} \right), \tag{4.15}$$

with [38]

$$C_{F_{2,q}}^{(1)} \left(x, \frac{Q^2}{\mu^2} \right) = P_{qq}^{(0)}(x) \ln \left(\frac{Q^2}{\mu^2} \right) + c_{F_{2,q}}^{(1)}(x) \tag{4.16}$$

$$\begin{aligned}
 & C_{F_{2,q}}^{(2)} \left(x, \frac{Q^2}{\mu^2} \right) = \frac{1}{2} \left\{ \left[P_{qq}^{(0)} \otimes P_{qq}^{(0)} \right] (x) - \beta_0 P_{qq}^{(0)} \right\} \ln^2 \left(\frac{Q^2}{\mu^2} \right) \\
 & \quad + \left\{ P_{qq}^{(1),\text{NS},+}(x) + \left[P_{qq}^{(0)} \otimes c_{F_{2,q}}^{(1)} \right] (x) - \beta_0 c_{F_{2,q}}^{(1)}(x) \right\} \ln \left(\frac{Q^2}{\mu^2} \right) \\
 & \quad + c_{F_{2,q}}^{(2)}(x). \tag{4.17}
 \end{aligned}$$

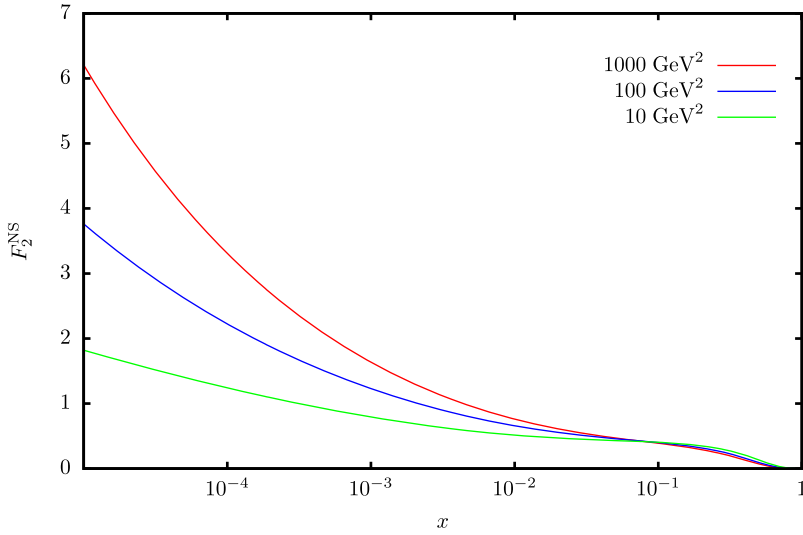


Fig. 15. The structure function F_2 due to photon exchange up to $O(\alpha_s^2)$ including the charm and bottom quark corrections in the on-shell scheme with $m_c = 1.59$ GeV [3] and $m_b = 4.78$ GeV [42] using the NNLO parton distribution functions [71].

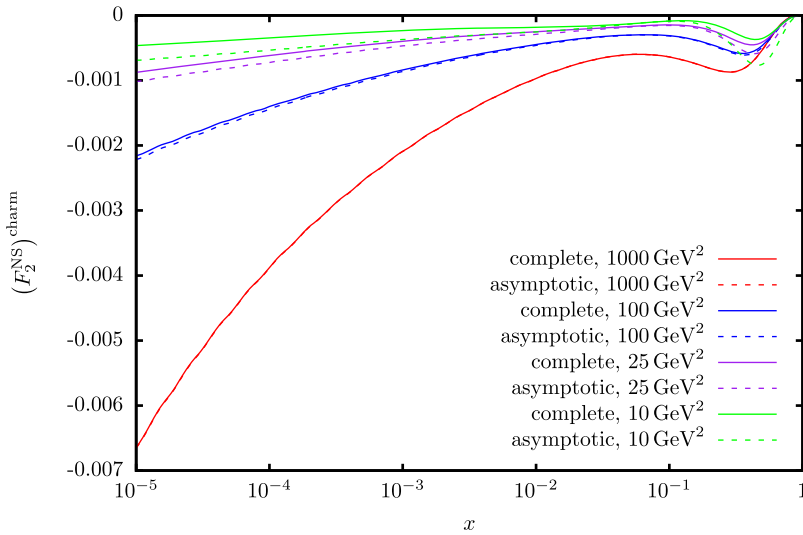


Fig. 16. The charm quark contribution to the structure function F_2 due to photon exchange up to $O(\alpha_s^2)$ as a function of x and Q^2 . The conditions are the same as in Fig. 15. Dashed lines: asymptotic representation in Q^2 for the heavy flavor corrections; full lines: complete heavy flavor contributions.

In Fig. 15 we show F_2^{NS} up to $O(\alpha_s^2)$ with the complete charm and bottom corrections. It rises for growing values of Q^2 for small values of x . The absolute charm and bottom quark corrections are illustrated in Figs. 16 and 17, illustrating as well the effect of the asymptotic results. They get close to the exact ones much earlier than in the case of F_L^{NS} .

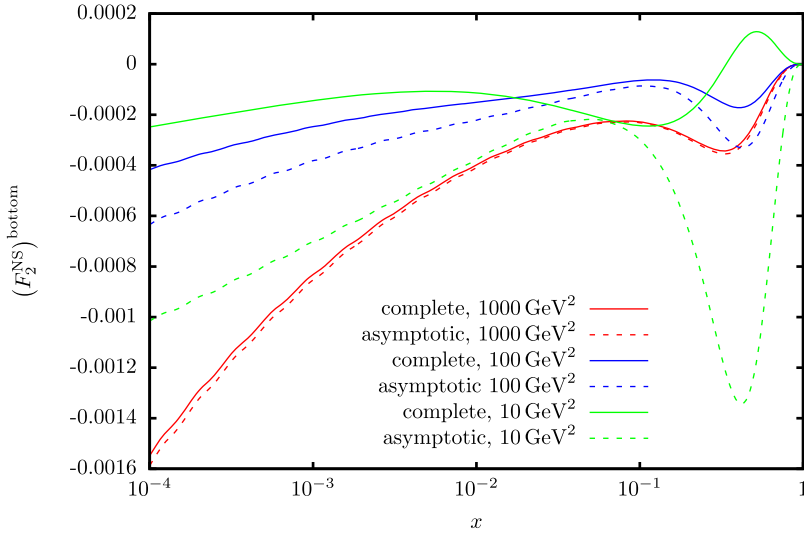


Fig. 17. The bottom quark contribution to the structure function F_2 due to photon exchange up to $O(\alpha_s^2)$ as a function of x and Q^2 . The conditions are the same as in Fig. 15. Dashed lines: asymptotic representation in Q^2 for the heavy flavor corrections; full lines: complete heavy flavor contributions.

The bottom quark contributions shown in Fig. 17 are about one order of magnitude smaller than those for charm quarks, still with clear differences between the exact and asymptotic result at $Q^2 \sim 100 \text{ GeV}^2$.

Fig. 18 illustrates the relative contribution of the heavy flavor corrections up to $O(\alpha_s^2)$. The corrections are rather flat in the small x region and amount to -0.1 to -0.6% for $x < 0.1$ growing towards -2.5% at large x from $Q^2 = 10 \text{ GeV}^2$ to 1000 GeV^2 .

5. The unpolarized non-singlet charged current structure functions

In the non-singlet charged current case we have to distinguish transitions between light flavors accompanied with heavy flavor production and the excitation of charm from massless down-type quarks. Due to the smallness of the corresponding CKM-matrix element [42] we will not consider the excitation of bottom quarks from the massless quarks. The current values of the contributing CKM-matrix elements are

$$\begin{aligned}
 |V_{ud}| &= 0.97425, & |V_{us}| &= 0.2253 \\
 |V_{cd}| &= 0.225, & |V_{cs}| &= 0.986.
 \end{aligned}
 \tag{5.1}$$

The corresponding flavor non-singlet combinations are given by

$$\begin{aligned}
 &F_1^{\bar{v}P}(x, Q^2) - F_1^{vP}(x, Q^2) \\
 &= \left[C_{F_{1,q}}^{\text{NS}} \left(x, \frac{Q^2}{\mu^2} \right) + L_{F_{1,q}}^{\text{NS}} \left(x, \frac{Q^2}{\mu^2}, \frac{m^2}{\mu^2} \right) \right] \otimes [(|V_{du}|^2 + |V_{su}|^2) \\
 &\quad \times u_v(x, \mu^2) - |V_{du}|^2 d_v(x, \mu^2)] - H_{F_{1,q}}^{\text{NS}} \left(x, \frac{Q^2}{\mu^2}, \frac{m^2}{\mu^2} \right) \otimes |V_{cd}|^2 d_v(x, \mu^2),
 \end{aligned}
 \tag{5.2}$$

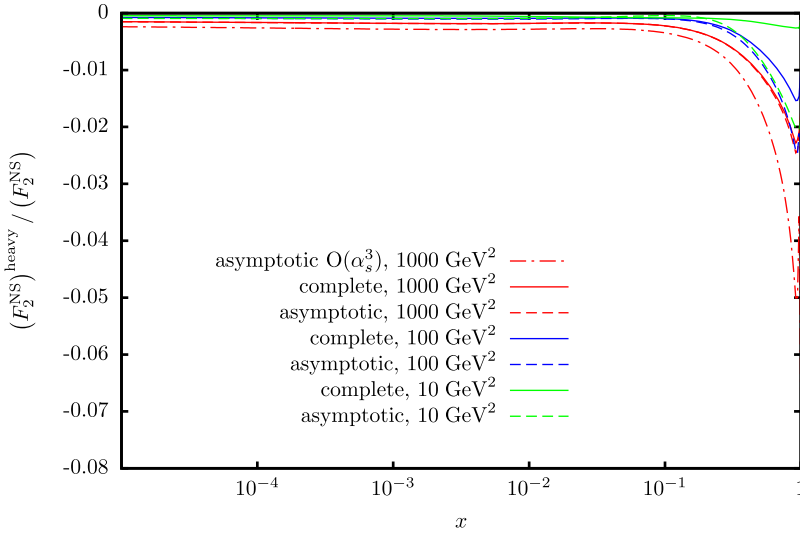


Fig. 18. The ratio of the heavy flavor contributions to the structure function F_2 due to photon exchange to the complete structure function up to $O(\alpha_s^2)$ as a function of x and Q^2 . The conditions are the same as in Fig. 15. Dashed lines: asymptotic representation in Q^2 for the heavy flavor corrections; full lines: complete heavy flavor contributions.

$$\begin{aligned}
 &F_2^{\bar{\nu}P}(x, Q^2) - F_2^{\nu P}(x, Q^2) \\
 &= 2x \left\{ \left[C_{F_2,q}^{\text{NS}} \left(x, \frac{Q^2}{\mu^2} \right) + L_{F_2,q}^{\text{NS}} \left(x, \frac{Q^2}{\mu^2}, \frac{m^2}{\mu^2} \right) \right] \otimes [(|V_{du}|^2 + |V_{su}|^2) \right. \right. \\
 &\quad \left. \left. \times u_v(x, \mu^2) - |V_{du}|^2 d_v(x, \mu^2) \right] - H_{F_2,q}^{\text{NS}} \left(x, \frac{Q^2}{\mu^2}, \frac{m^2}{\mu^2} \right) \otimes |V_{cd}|^2 d_v(x, \mu^2) \right\}, \quad (5.3)
 \end{aligned}$$

$$\begin{aligned}
 &F_3^{\bar{\nu}P}(x, Q^2) + F_3^{\nu P}(x, Q^2) \\
 &= 2 \left\{ \left[C_{F_3,q}^{\text{NS}} \left(x, \frac{Q^2}{\mu^2} \right) + L_{F_3,q}^{\text{NS}} \left(x, \frac{Q^2}{\mu^2}, \frac{m^2}{\mu^2} \right) \right] \otimes [|V_{du}|^2 d_v(x, \mu^2) \right. \right. \\
 &\quad \left. \left. + (|V_{du}|^2 + |V_{su}|^2) u_v(x, \mu^2) \right] + H_{F_3,q}^{\text{NS}} \left(x, \frac{Q^2}{\mu^2}, \frac{m^2}{\mu^2} \right) \otimes |V_{cd}|^2 d_v(x, \mu^2) \right\}. \quad (5.4)
 \end{aligned}$$

Here, $C_{F_i,q}^{\text{NS}}$, $L_{F_i,q}^{\text{NS}}$, and $H_{F_i,q}^{\text{NS}}$ denote the massless (C) and massive Wilson coefficients (L, H) for the coupling of the weak bosons to only massless quarks (C, L) and for charm excitation (H). We assume that the sea quark distributions obey

$$u_s(x, \mu^2) = \bar{u}(x, Q^2), \quad d_s(x, \mu^2) = \bar{d}(x, Q^2), \quad s(x, \mu^2) = \bar{s}(x, Q^2). \quad (5.5)$$

The contributions due to the Wilson coefficients $H_{F_i,q}^{\text{NS}}$, $i = 1, 2, 3$ are Cabibbo suppressed.

The combinations (5.2)–(5.4) are related to the unpolarized Bjorken sum rule [24], the Adler sum rule [23], and the Gross–Llewellyn Smith sum rule [26], respectively, by their first moments. First we consider these combinations themselves and turn to the sum rules later. Up to $O(\alpha_s)$ the single heavy quark excitations have been calculated in Refs. [34,35] correcting results in [36].

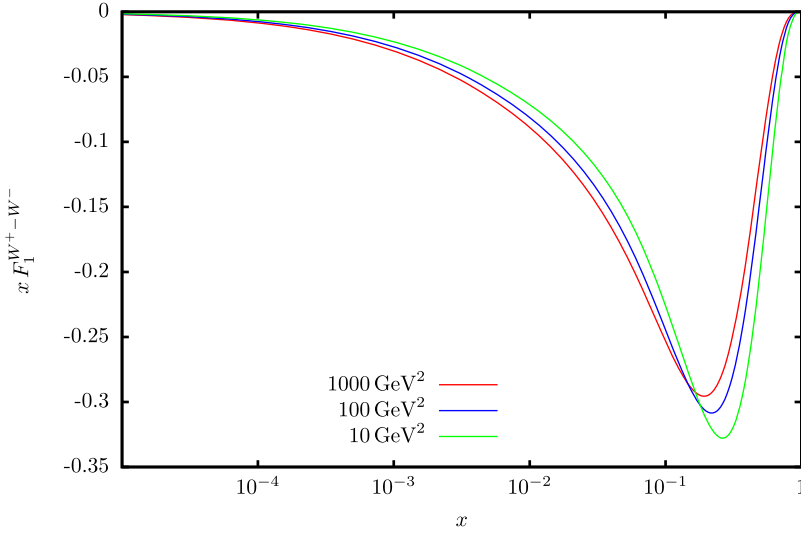


Fig. 19. The charged current structure function $x F_1^{W^+-W^-}$ up to $O(\alpha_s^2)$ including the charm quark corrections in the on-shell scheme with $m_c = 1.59$ GeV [3] and using the NNLO parton distribution functions [71].

At two-loop order, only the asymptotic results for $Q^2 \gg m^2$ are available [18],⁹ to which we refer in the following. We will limit our considerations to the case of the charm contributions.

In Fig. 19 we illustrate the non-singlet structure function $x F_1^{W^+-W^-}$ up to $O(\alpha_s^2)$, showing its scaling violations in the range $Q^2 = 10$ to 1000 GeV². Its charm quark corrections up to $O(\alpha_s^2)$, using the asymptotic corrections for the $O(\alpha_s^2)$ term of the flavor excitation contributions as a first approximation, are illustrated in Figs. 20–22 for virtualities $Q^2 = 4, 10$ and 100 GeV².

The higher order results lower the corrections in the small x region and enlarge it at large x . The asymptotic corrections work well in the whole region $Q^2 \in [4, 100]$ GeV² for small values of x and in the whole region at $Q^2 = 100$ GeV². The relative corrections amount to values between 0 and -8% .

In Fig. 23 the charged current structure function $F_2^{W^+-W^-}$ is shown, including the charm quark corrections. Again QCD-evolution moves the profile towards smaller values of x . The relative corrections due to charm are shown in Figs. 24–26 for the scales $Q^2 = 4, 10$ and 100 GeV².

Here we also compare the asymptotic result against the complete ones. The charm contribution is found in the range of 0 to $\sim -12\%$ at $Q^2 = 4$ GeV² to 0 to $\sim -8\%$, at $Q^2 = 100$ GeV² peaking around $x \sim 0.03$.

In Fig. 27 the charged current structure function $x F_3^{W^+-W^-}$ including the charm quark corrections are shown. In this case also the asymptotic 3-loop corrections have been calculated [17]. As shown in Figs. 28–30, the charm quark corrections vary from $\sim +2\%$ to -2% from small to large x . With rising values of Q^2 the corrections become more pronounced at large values of x . Note that the asymptotic $O(\alpha_s^3)$ corrections yield significant contributions both at small and large values of x .

⁹ A sign error in [22] has been corrected.

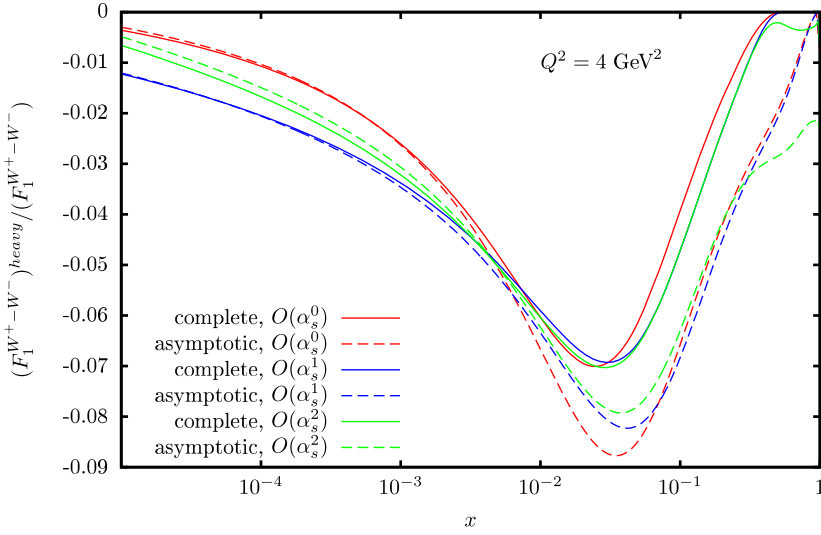


Fig. 20. The ratio of the charm quark contributions to the charged current structure function $x F_1^{W^+-W^-}$ up to $O(\alpha_s^2)$ to the full corrections at $Q^2 = 4 \text{ GeV}^2$. The other conditions are the same as in Fig. 19.

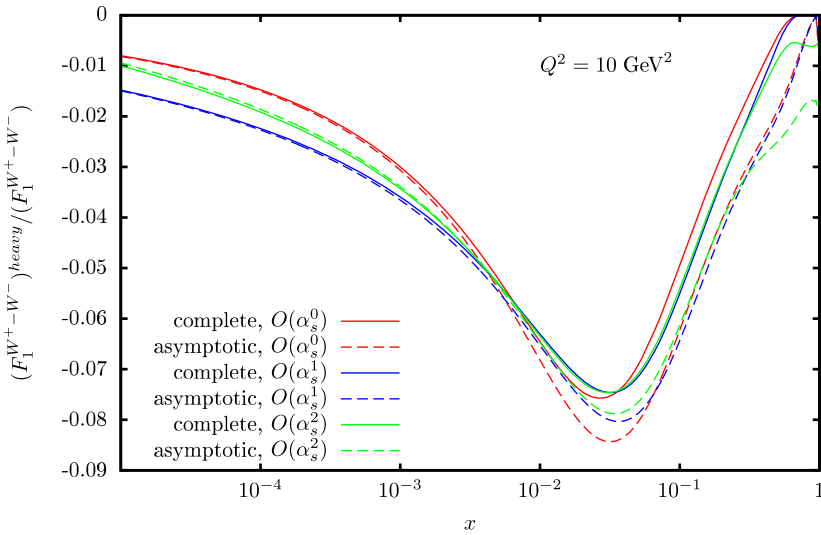


Fig. 21. The ratio of the charm quark contributions to the charged current structure function $x F_1^{W^+-W^-}$ up to $O(\alpha_s^2)$ to the full corrections at $Q^2 = 10 \text{ GeV}^2$. The other conditions are the same as in Fig. 19.

6. The sum rules

In the following we discuss the corrections to the Adler sum rule [23], which have to vanish, and calculate the corrections to the polarized Bjorken sum rule [25], the unpolarized Bjorken sum rule [24], and the Gross–Llewellyn Smith sum rule [26], which are obtained as the first moments of the massive Wilson coefficients calculated in the previous sections. The combination of the

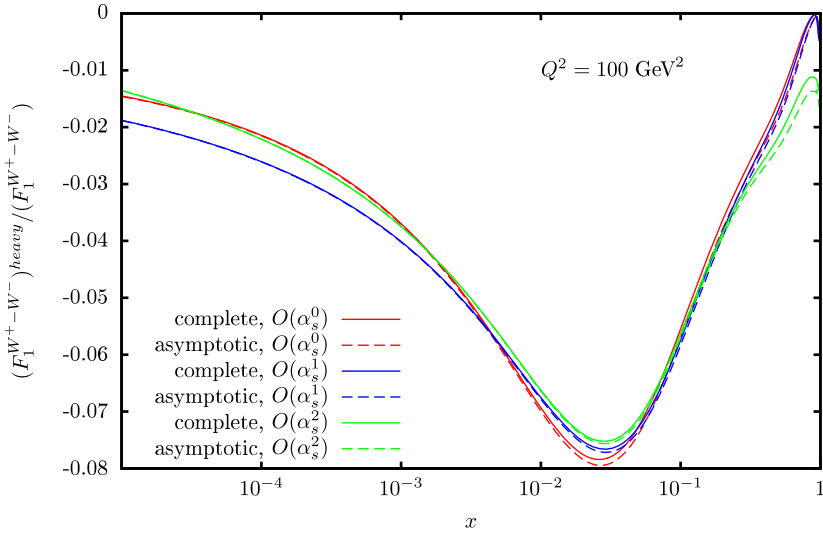


Fig. 22. The ratio of the charm quark contributions to the charged current structure function $x F_1^{W^+-W^-}$ up to $O(\alpha_s^2)$ to the full corrections at $Q^2 = 100 \text{ GeV}^2$. The other conditions are the same as in Fig. 19.

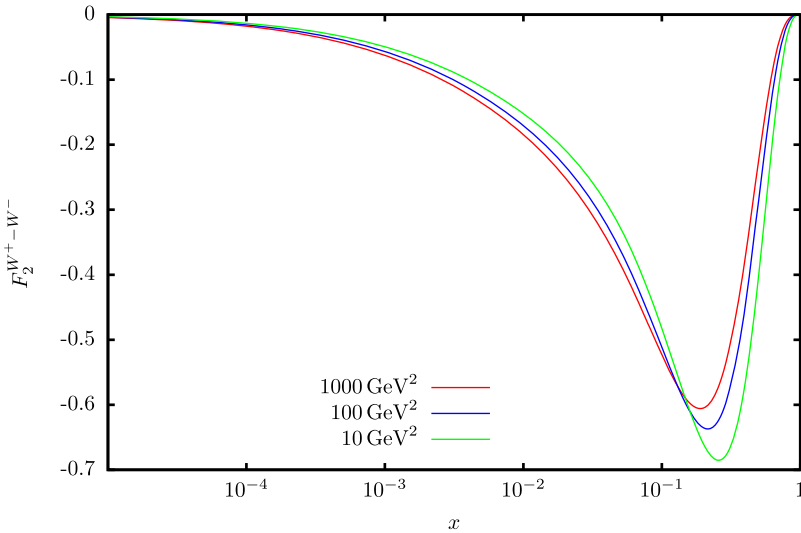


Fig. 23. The charged current structure function $F_2^{W^+-W^-}$ up to $O(\alpha_s^2)$ including the charm quark corrections in the on-shell scheme with $m_c = 1.59 \text{ GeV}$ [3] and using the NNLO parton distribution functions [71].

parton distributions is partly different, as here differences between structure functions in the neutral current case are considered. But this affects only the normalization factor of the sum rules, which are known constants. As has been outlined in Refs. [16,17] up to 3-loop order, in the asymptotic region $Q^2 \gg m^2$ the sum rules only modify the massless approximation by replacing the number of massless flavors from $N_F \rightarrow N_F + 1$. Given the factorization of the massive Wilson coefficients [8,9], this holds for all orders in the coupling constant, since the first

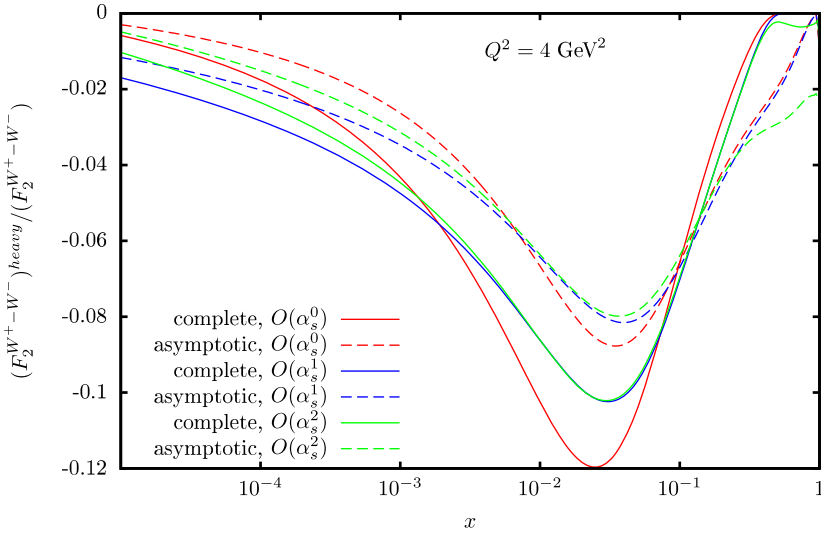


Fig. 24. The ratio of the charm quark contributions to the charged current structure function $F_2^{W^+-W^-}$ up to $O(\alpha_s^2)$ to the full corrections at $Q^2 = 4 \text{ GeV}^2$. The other conditions are the same as in Fig. 23.

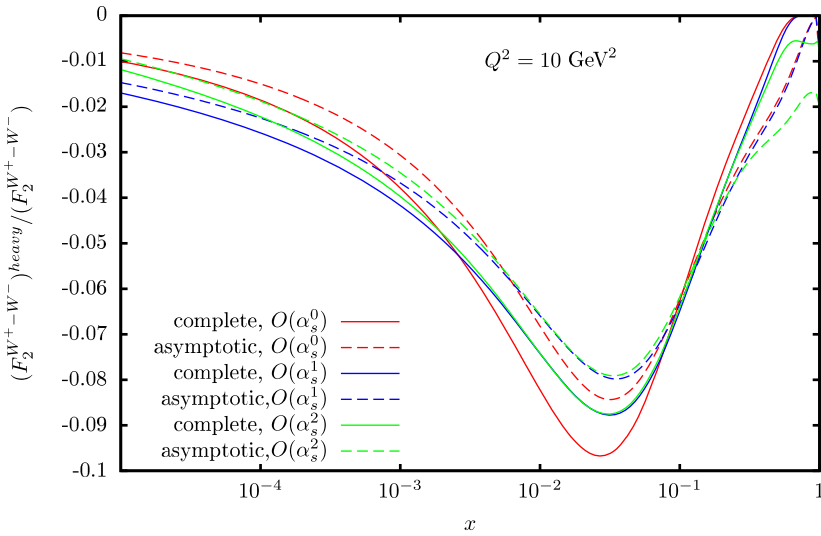


Fig. 25. The ratio of the charm quark contributions to the charged current structure function $F_2^{W^+-W^-}$ up to $O(\alpha_s^2)$ to the full corrections at $Q^2 = 10 \text{ GeV}^2$. The other conditions are the same as in Fig. 23.

moment of the massive non-singlet OMEs vanish order by order in the coupling constant due to fermion number conservation. The 4-loop corrections to these sum rules have been calculated in Refs. [73–75]. Earlier Padé estimates were given in [76].

We emphasize that in the present paper the inclusive Wilson coefficients are calculated for deep-inelastic scattering, but not those in the flavor tagged case. The relations obtained do not smoothly transform into the photo-production limit $Q^2 \approx 0$, both for the Wilson coefficients and

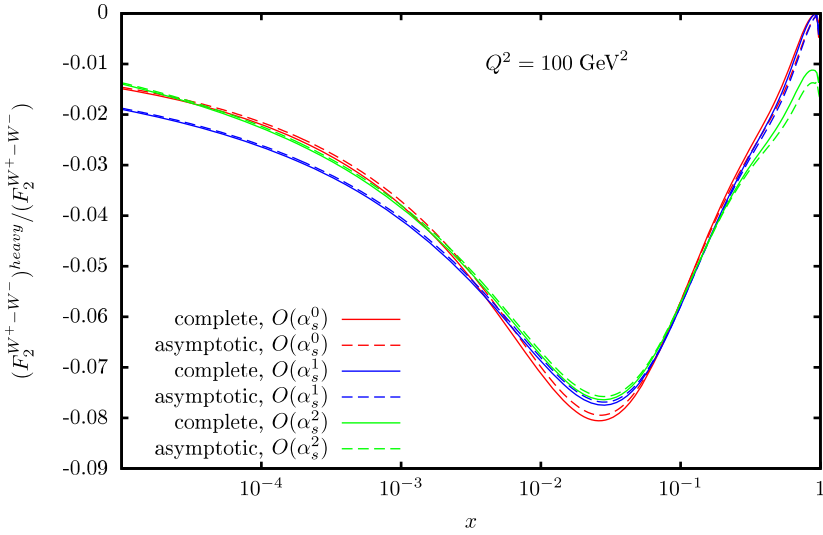


Fig. 26. The ratio of the charm quark contributions to the charged current structure function $F_2^{W^+-W^-}$ up to $O(\alpha_s^2)$ to the full corrections at $Q^2 = 100 \text{ GeV}^2$. The other conditions are the same as in Fig. 23.

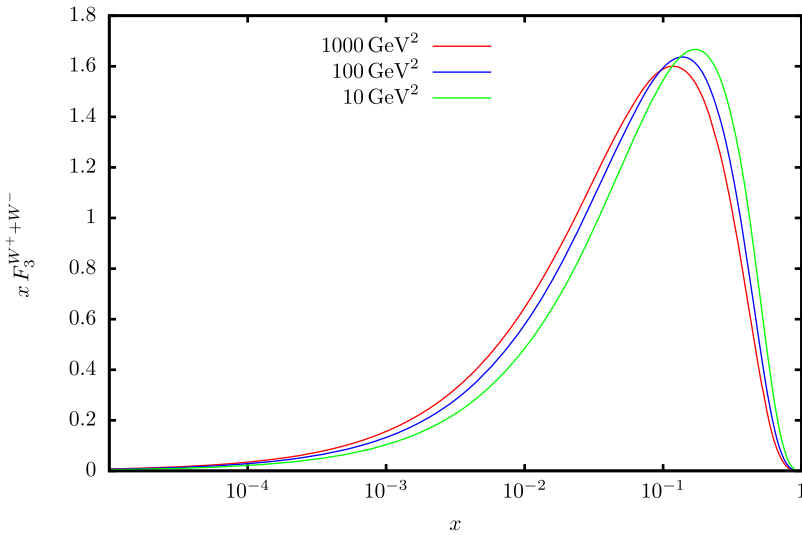


Fig. 27. The charged current structure function $x F_3^{W^++W^-}$ up to $O(\alpha_s^2)$ including the charm quark corrections in the on-shell scheme with $m_c = 1.59 \text{ GeV}$ [3] and using the NNLO parton distribution functions [71].

the parton distribution functions, setting $\mu^2 = Q^2$. They are valid only up to a lower scale Q_0^2 , which usually should be at least of $O(m_c^2)$ or larger, also to stay outside the region of higher twist corrections. In the case of the sum rules discussed below, in the limit $Q^2/m^2 \rightarrow 0$ logarithmic contributions survive, while this is not the case in the limit of large virtualities $m^2/Q^2 \rightarrow 0$. The photo-production region for the corresponding structure functions needs a separate treatment.

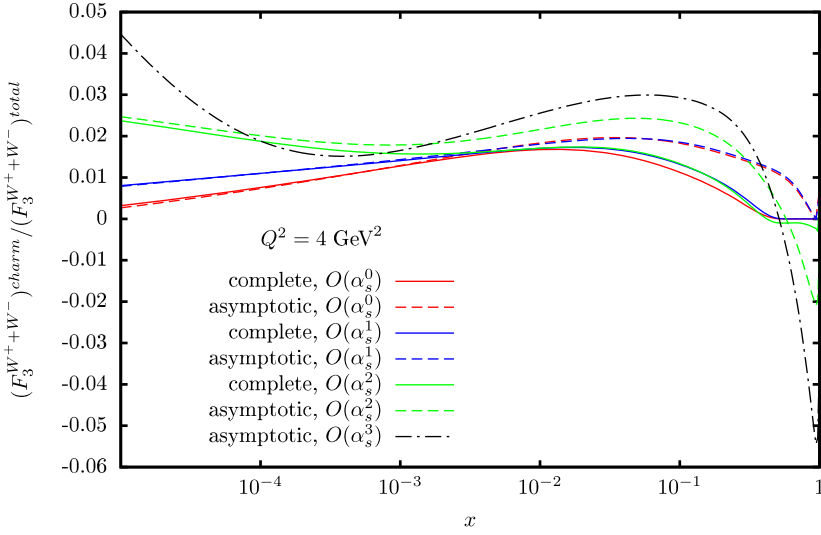


Fig. 28. The ratio of the charm quark contributions to the charged current structure function $x F_3^{W^+ + W^-}$ up to $O(\alpha_s^2)$ to the full corrections at $Q^2 = 4 \text{ GeV}^2$. Dash-dotted line: corrections to $O(\alpha_s^3)$ in the asymptotic case. The other conditions are the same as in Fig. 23.

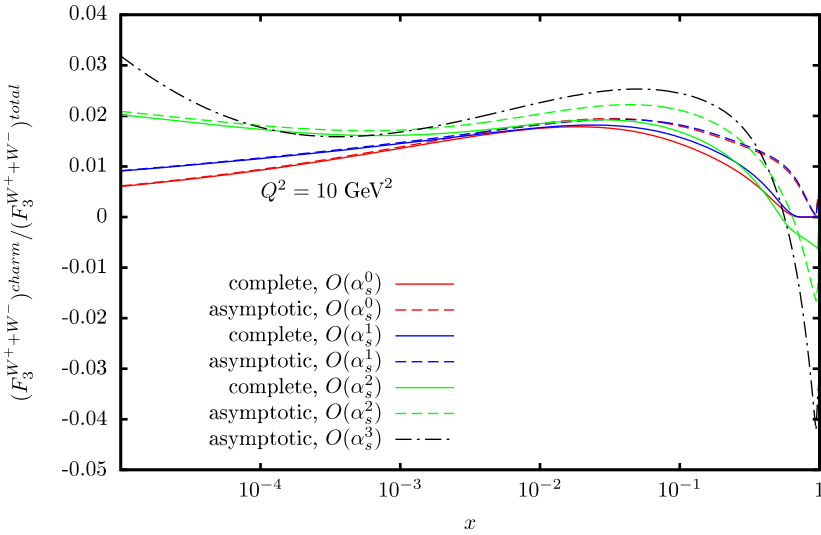


Fig. 29. The ratio of the charm quark contributions to the charged current structure function $x F_3^{W^+ + W^-}$ up to $O(\alpha_s^2)$ to the full corrections at $Q^2 = 10 \text{ GeV}^2$. Dash-dotted line: corrections to $O(\alpha_s^3)$ in the asymptotic case. The other conditions are the same as in Fig. 23.

In the following we will discuss the complete massive corrections to the four sum rules in the deep-inelastic region. The power corrections of a single heavy quark c or b will be shown to basically interpolate between N_F and $N_F + 1$ massless flavors in the limit $m^2/Q^2 \rightarrow 0$, while at lower scales Q^2 , partly negative virtual corrections are possible. The sum rules are observables and we represent them choosing the factorization scale $\mu^2 = Q^2$. The scale matching can be

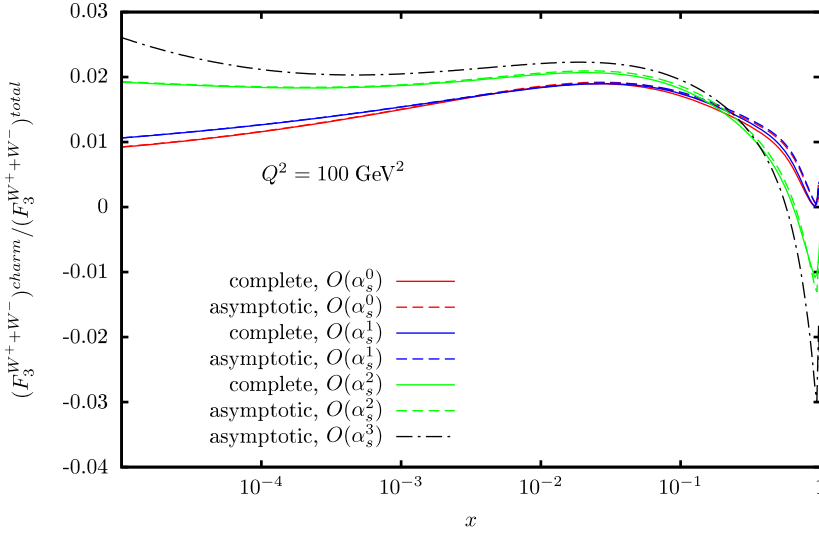


Fig. 30. The ratio of the charm quark contributions to the charged current structure function $x F_3^{W^+ + W^-}$ up to $O(\alpha_s^2)$ to the full corrections at $Q^2 = 100 \text{ GeV}^2$. Dash-dotted line: corrections to $O(\alpha_s^3)$ in the asymptotic case. The other conditions are the same as in Fig. 23.

performed analytically in Mellin space up to the respective order in a_s in which the quantity is calculated, cf. [31].

To get closer to the unitary representation for the CKM matrix elements, we calculate the functions $H_{F_{i,q}}$, (2.8), (2.9), allowing for massive charm quarks to be pair produced also for this Cabibbo suppressed term, but referring to massless $s \rightarrow c$ charged current transitions for the real and virtual corrections.

Finally, we also consider the target mass corrections to the deep-inelastic sum rules, as they are of relevance in the region of lower values of Q^2 .

6.1. The Adler sum rule

The Adler sum rule [23] states

$$\int_0^1 \frac{dx}{x} \left[F_2^{\bar{\nu}p}(x, Q^2) - F_2^{\nu p}(x, Q^2) \right] = 2[1 + \sin^2(\theta_c)] \tag{6.1}$$

for three massless flavors. Here θ_c denotes the Cabibbo angle [33]. The integral (6.1) neither receives QCD nor quark- or target mass corrections, cf. also [65,77].

The Compton contribution yields

$$\int_0^z dz L_{F_{2,q}}^{\text{NS},(2),C}(z) = a_s^2 C_F T_F \left\{ -\frac{2426}{81} - \frac{476}{9} \tilde{\lambda}^2 + \left(\frac{400}{27} + \frac{220}{9} \tilde{\lambda}^2 \right) \ln(\xi) \right. \\ \left. - \left[\frac{20}{3} \tilde{\lambda} + \frac{92}{9} \tilde{\lambda}^3 \right] \left[\text{Li}_2 \left(-\frac{1-\tilde{\lambda}}{1+\tilde{\lambda}} \right) - \text{Li}_2 \left(-\frac{1+\tilde{\lambda}}{1-\tilde{\lambda}} \right) \right] \right\}$$

$$-\left[\frac{10}{3} + 4\tilde{\lambda}^2 - 2\tilde{\lambda}^4\right] \left[\text{Li}_3\left(-\frac{1-\tilde{\lambda}}{1+\tilde{\lambda}}\right) + \text{Li}_3\left(-\frac{1+\tilde{\lambda}}{1-\tilde{\lambda}}\right) - 2\zeta_3 \right], \tag{6.2}$$

which is canceled by the virtual correction $\int_0^1 dz L_{F_{2,q}}^{\text{NS},(2),V}(z)$, (3.12). The first moment of the contribution with massless final states

$$L_{F_{2,q}}^{\text{NS},(2),\text{massive}}\left(\frac{Q^2}{m^2}, \frac{m^2}{\mu^2}z\right) = -a_s^2 \beta_0 \ln\left(\frac{m^2}{\mu^2}\right) \left[P_{qq}^{(0)}(z) \ln\left(\frac{Q^2}{\mu^2}\right) + c_{F_{2,q}}^{(1)}(z) \right], \tag{6.3}$$

also vanishes, cf. (4.13), (3.6).

For the charged current flavor excitation slow rescaling at tree level yields

$$\begin{aligned} \int_0^1 dx \frac{F_2^{\bar{v}p}(x, Q^2) - F_2^{vp}(x, Q^2)}{x} &= \int_0^{\frac{1+\xi}{\xi}} \frac{dz}{z} \left[F_2^{\bar{v}p}(z, Q^2) - F_2^{vp}(z, Q^2) \right] \\ &= \int_0^1 \frac{dz}{z} \left[F_2^{\bar{v}p}(z, Q^2) - F_2^{vp}(z, Q^2) \right], \end{aligned} \tag{6.4}$$

since the support of $F_2(z, Q^2)$ is $z \in [0, 1]$. For the first order massive QCD corrections given in [34,35] the first moment (6.1) vanishes. The corresponding $O(\alpha_s^2)$ corrections have only been studied in the asymptotic case [18] and vanish. For massless quarks, the Adler sum rule has been checked at $O(\alpha_s^3)$ in [78]. It seems that in the case of massless 4-loop corrections, the validity of the sum rule has not yet been checked perturbatively [79]. The target mass corrections are studied in Section 6.5.

In contrast, the QCD-, quark mass- and target mass corrections to the first moments of the structure functions g_1 , F_1 and F_3 do not vanish.

6.2. The polarized Bjorken sum rule

The polarized Bjorken sum rule [25] refers to the first moment of the flavor non-singlet combination

$$\int_0^1 dx \left[g_1^{ep}(x, Q^2) - g_1^{en}(x, Q^2) \right] = \frac{1}{6} \left| \frac{g_A}{g_V} \right| C_{\text{pBJ}}(\hat{a}_s), \tag{6.5}$$

with $g_{A,V}$ the neutron decay constants, $g_A/g_V \approx -1.2767 \pm 0.0016$ [80] and

$$\hat{a}_s = \frac{\alpha_s}{\pi}. \tag{6.6}$$

The 1- [40], 2- [81], 3- [82] and 4-loop QCD corrections [75] in the massless case are given by

$$\begin{aligned} C_{\text{pBJ}}(\hat{a}_s) &= 1 - \hat{a}_s + \hat{a}_s^2(-4.58333 + 0.33333N_F) \\ &\quad + \hat{a}_s^3(-41.4399 + 7.60729N_F - 0.17747N_F^2) \\ &\quad + \hat{a}_s^4(-479.448 + 123.391N_F - 7.69747N_F^2 + 0.10374N_F^3) \Big|_{\text{NS}} \\ &\quad + \hat{a}_s^4(12.2222 - 0.740741N_F) \Big|_{\text{SI}} \sum_{k=1}^{N_F} e_k \end{aligned} \tag{6.7}$$

choosing the renormalization scale $\mu^2 = Q^2$, cf. [41] for $SU(3)_c$. Here N_F denotes the number of active light flavors and the labels NS and SI refer to the genuine ‘non-singlet’ and ‘singlet’ contributions, respectively. The expression for general color factors was given in Refs. [75,83].¹⁰ The massless corrections for $N_F = 3$ and $N_F = 4$ are

$$C_{\text{pBJ}}(N_F = 3) = 1 - \hat{a}_s - 3.58334\hat{a}_s^2 - 20.2153\hat{a}_s^3 - 175.781\hat{a}_s^4 \quad \text{and} \quad (6.8)$$

$$C_{\text{pBJ}}(N_F = 4) = 1 - \hat{a}_s - 3.25001\hat{a}_s^2 - 13.8503\hat{a}_s^3 - 98.2889\hat{a}_s^4. \quad (6.9)$$

For the asymptotic massive corrections (2.7)–(2.8) only the first moments of the massless Wilson coefficients $\hat{C}_{g_1,q}^{(2,3),\text{NS}}(N_F)$ contribute, since the first moments of the massive non-singlet OMEs vanish due to fermion number conservation, a property holding even at higher order. Therefore, any new heavy quark changes Eq. (6.7) by a shift in $N_F \rightarrow N_F + 1$ only, for the asymptotic corrections.

We turn now to the heavy quark corrections, which are given by

$$C_{\text{pBJ}}^{\text{massive,(2)}} = 3C_F T_F \left\{ \frac{6\xi^2 + 2735\xi + 11724}{5040\xi} - \frac{\sqrt{\xi + 4} (3\xi^3 + 106\xi^2 + 1054\xi + 4812)}{\xi^{3/2} 5040} \right. \\ \left. \times \ln \left[\frac{\sqrt{1 + \frac{4}{\xi}} + 1}{\sqrt{1 + \frac{4}{\xi}} - 1} \right] - \frac{1}{\xi^2} \frac{5}{12} \ln^2 \left[\frac{\sqrt{1 + \frac{4}{\xi}} + 1}{\sqrt{1 + \frac{4}{\xi}} - 1} \right] + \frac{(3\xi^2 + 112\xi + 1260)}{5040} \ln(\xi) \right\}, \quad (6.10)$$

see Appendix C. In the asymptotic region $\xi \gg 1$, $C_{\text{pBJ}}^{\text{massive,(2)}}$ behaves like

$$C_{\text{pBJ}}^{\text{massive,(2)}} \propto 3C_F T_F \left\{ \frac{1}{2} - \frac{5}{12\xi^2} \ln^2(\xi) - \frac{4}{3\xi} \ln(\xi) + \frac{17}{9\xi} + O\left(\frac{\ln(\xi)}{\xi^2}\right) \right\}. \quad (6.11)$$

Up to 2-loop order the massless and the massive corrections to the polarized Bjorken sum rule are given by

$$C_{\text{pBJ}}(\xi_c) = 1 - \hat{a}_s - \hat{a}_s^2 \left\{ -\frac{55}{12} + \frac{1}{3} \left[N_F + C_{\text{pBJ}}^{\text{massive,(2)}}(\xi_c) + C_{\text{pBJ}}^{\text{massive,(2)}} \left(\xi_c \frac{m_c^2}{m_b^2} \right) \right] \right\} \\ + O(\hat{a}_s^3), \quad (6.12)$$

accounting for the charm and bottom quark contributions, with $\xi_c = Q^2/m_c^2$. In Fig. 31 the effect of the heavy flavor Wilson coefficients $C_{\text{pBJ}}^{\text{massive,(2)}}$ for charm and bottom are illustrated as a function of ξ_c .

At low scales the corrections are negative and the interpolation to the asymptotic value 2 for $N_F \rightarrow N_F + 2$ in ξ_c proceeds very slowly. In Table 1 we illustrate the mass effects for the 2-loop terms. The massless prediction is only reached for considerably large values of Q^2 , namely for $\xi_c \sim 24$ in the case of $N_F = 4$ and $\xi_c \gg 500$ for $N_F = 5$.

In Table 2 we compare the values of the polarized Bjorken sum rule for different values of Q^2 to illustrate the effect of the heavy flavor contribution. The massive contribution turns out to

¹⁰ An estimate of the singlet contribution has been made in Ref. [84]. We refer to the result of the calculation in Ref. [83].

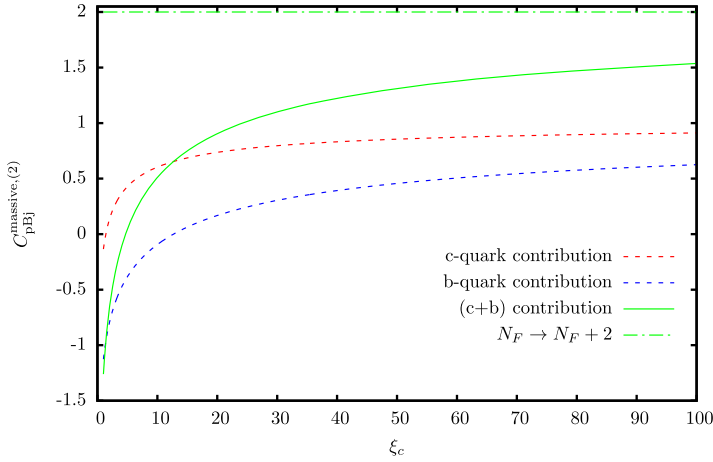


Fig. 31. The $O(a_s^2)$ coefficients $C_{\text{pBJ}}^{\text{massive},(2)}$ for charm and bottom quarks as a function of ξ_c .

Table 1

The massless and massive 2-loop corrections to the Bjorken sum rule as a function of ξ_c . We also indicated the respective purely massless results for $N_F = 3, 4$ and 5.

$\xi = 1$	-4.003
$N_F = 3$	-3.583
$\xi = 5$	-3.569
$\xi = 10$	-3.413
$\xi = 24$	-3.251
$N_F = 4$	-3.250
$\xi = 50$	-3.146
$\xi = 100$	-3.071
$\xi = 500$	-2.970
$N_F = 5$	-2.917

Table 2

Comparison of C_{pBJ} in the massless approximation to $O(\hat{a}_s^4)$, $O(\hat{a}_s^3)$ for $N_F = 3$ massless flavors, and the $O(\hat{a}_s^2)$ contributions due to charm and bottom.

Q^2/GeV^2	$O(\hat{a}_s^4)$ massless	$O(\hat{a}_s^3)$ massless	Δ_{4-3}	Massive $O(\hat{a}_s^2)$
30	0.9180	0.9205	-0.0025	-0.0008
100	0.9321	0.9335	-0.0014	-0.0011
10000	0.9587	0.9590	-0.0003	-0.0008

be comparable in size to the massless 4-loop contribution. Due to surviving logarithms in ξ in the large ξ region in the tagged flavor case, different results are obtained [27,28]. However, the corresponding quantity does not describe the heavy flavor contributions to the structure functions, which are inclusive quantities.

6.3. The unpolarized Bjorken sum rule

The unpolarized Bjorken sum rule [24] is given by

$$\int_0^1 dx \left[F_1^{\bar{\nu}P}(x, Q^2) - F_1^{\nu P}(x, Q^2) \right] = C_{\text{uBJ}}(\hat{a}_s). \tag{6.13}$$

The massless 1- [72,85–87], 2-loop [81], 3-loop [88] and 4-loop [73] QCD corrections have been calculated

$$\begin{aligned} C_{\text{uBJ}}(\hat{a}_s) = & 1 - 0.66667\hat{a}_s + \hat{a}_s^2(-3.83333 + 0.29630N_F) \\ & + \hat{a}_s^3(-36.1549 + 6.33125N_F - 0.15947N_F^2) \\ & + \hat{a}_s^4(-436.768 + 111.873N_F - 7.11450N_F^2 + 0.10174N_F^3), \end{aligned} \tag{6.14}$$

setting $\mu^2 = Q^2$ for $SU(3)_c$. For $N_F = 3, 4$ the massless QCD corrections are given by

$$C_{\text{uBJ}}(\hat{a}_s, N_F = 3) = 1 - 0.66667\hat{a}_s - 2.94444\hat{a}_s^2 - 18.5963\hat{a}_s^3 - 162.436\hat{a}_s^4 \tag{6.15}$$

$$C_{\text{uBJ}}(\hat{a}_s, N_F = 4) = 1 - 0.66667\hat{a}_s - 2.64815\hat{a}_s^2 - 13.3813\hat{a}_s^3 - 96.6032\hat{a}_s^4. \tag{6.16}$$

The massive corrections start at $O(\alpha_s^0)$ with the $s' \rightarrow c$ transitions [34,35]

$$C_{\text{uBJ}}^{\text{massive},(0)}(\xi) = \frac{\xi}{1 + \xi} \tag{6.17}$$

$$C_{\text{uBJ}}^{\text{massive},(1)}(\xi) = C_F \frac{1}{4} \left\{ \frac{2 + \xi - 2\xi^2}{\xi(1 + \xi)} - 2 \frac{1 + \xi - 3\xi^2}{\xi^2(1 + \xi)} \ln(1 + \xi) \right\}. \tag{6.18}$$

$C_{\text{uBJ}}^{\text{massive},(1)}(\xi)$ approaches the asymptotic value of $-2/3$ given in (6.14). Its behavior as a function of ξ_c is shown in Fig. 32.

The massive 2-loop corrections are given by

$$\begin{aligned} C_{\text{uBJ}}^{\text{massive},(2)}(\xi) = & \hat{a}_s^2 C_F T_F \frac{1}{16} \left\{ -\frac{8}{\xi^2} \ln^2 \left(\frac{\sqrt{1 + \frac{4}{\xi}} + 1}{\sqrt{1 + \frac{4}{\xi}} - 1} \right) + \ln \left(\frac{\sqrt{1 + \frac{4}{\xi}} + 1}{\sqrt{1 + \frac{4}{\xi}} - 1} \right) \right. \\ & \times \left[-\frac{344}{21\xi} - \frac{268}{105} - \frac{4\xi}{105} + \frac{2\xi^2}{105} \right] \sqrt{1 + \frac{4}{\xi}} \\ & \left. + \left(\frac{8}{3} - \frac{2\xi^2}{105} \right) \ln(\xi) + \frac{856}{21\xi} + \frac{2258}{315} - \frac{4\xi}{105} \right\}. \end{aligned} \tag{6.19}$$

In the region $\xi \gg 1$ one obtains

$$C_{\text{uBJ}}^{\text{massive},(2)}(\xi) \approx \hat{a}_s^2 C_F T_F \left\{ \frac{4}{9} + \frac{1}{\xi} \left[\frac{20}{9} - \frac{4}{3} \ln(\xi) \right] \right\} + O \left(\frac{\ln^2(\xi)}{\xi^2} \right). \tag{6.20}$$

In Fig. 33, $C_{\text{uBJ}}^{\text{massive},(2)}(\xi)$ is shown as a function of ξ .

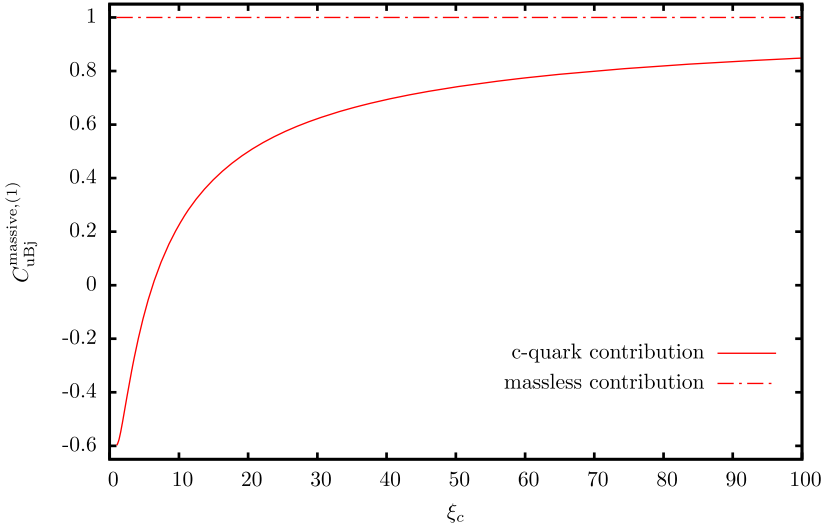


Fig. 32. The $O(a_s)$ coefficient $C_{\text{uBJ}}^{\text{massive},(1)}$ as a function of ξ_c , normalized to 1 in the limit $\xi_c \rightarrow \infty$.

Table 3

Comparison of C_{uBJ} in the massless approximation to $O(\hat{a}_s^4)$, $O(\hat{a}_s^2)$ for $N_F = 3$ massless flavors, and the $O(\hat{a}_s^2)$ contributions due to charm.

Q^2/GeV^2	$O(\hat{a}_s^4)$ massless	$O(\hat{a}_s^3)$ massless	Δ_{4-3}	Massive
30	0.9414	0.9437	-0.0023	0.0032
100	0.9520	0.9533	-0.0013	0.0014
10000	0.9714	0.9717	-0.0003	0.0004

To $O(\hat{a}_s^2)$ the unpolarized Bjorken sum rule reads

$$C_{\text{uBJ}}(\xi) = \left[1 - |V_{cd}|^2 \left[C_{\text{uBJ}}^{\text{charm},(0)}(\xi) - 1 \right] \right] - \hat{a}_s \left\{ \frac{2}{3} + |V_{cd}|^2 \left[C_{\text{uBJ}}^{\text{charm},(1)}(\xi) + \frac{2}{3} \right] \right\} + \hat{a}_s^2 \left[-\frac{23}{6} + \frac{8}{27} N_F + C_{\text{uBJ}}^{\text{charm},(2)}(\xi) \right] + O(\hat{a}_s^3). \tag{6.21}$$

In Table 3 we compare the values of the unpolarized Bjorken sum rule for different values of Q^2 to illustrate the effect of the heavy flavor contribution.

The charm corrections at $O(\hat{a}_s^2)$ are of the same size as the massless $O(\hat{a}_s^4)$ corrections.

6.4. The Gross–Llewellyn Smith sum rule

The Gross–Llewellyn Smith sum rule [26] refers to the first moment of the flavor non-singlet combination

$$\int_0^1 dx \left[F_3^{\bar{\nu}p}(x, Q^2) + F_3^{\nu p}(x, Q^2) \right] = 6C_{\text{GLS}}(\hat{a}_s), \tag{6.22}$$

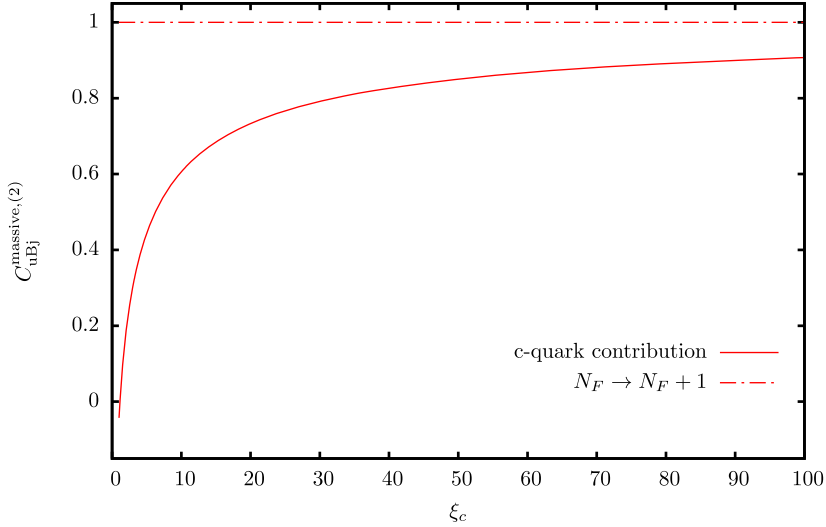


Fig. 33. The $O(a_s^2)$ coefficient $C_{\text{uBJ}}^{\text{massive},(2)}$ as a function of ξ_c , normalized to 1 in the limit $\xi_c \rightarrow \infty$.

assuming idealized CKM mixing. The 1-loop [72,85–87], 2-loop [81], 3-loop [82] and 4-loop QCD corrections [74,75] in the massless case are given by

$$\begin{aligned}
 C_{\text{GLS}}(\hat{a}_s) &= 1 - \hat{a}_s + \hat{a}_s^2(-4.58333 + 0.33333N_F) \\
 &\quad + \hat{a}_s^3(-41.4399 + 8.02047N_F - 0.17747N_F^2) \\
 &\quad + \hat{a}_s^4(-479.448 + 129.193N_F - 7.93065N_F^2 + 0.10374N_F^3), \tag{6.23}
 \end{aligned}$$

choosing the renormalization scale $\mu^2 = Q^2$ for $SU(3)_c$. The expression for general color factors was given in Refs. [74,75]. Note that the QCD corrections to the Gross–Llewellyn Smith sum rule and to the polarized Bjorken sum rule [25] are identical up to $O(\hat{a}_s^2)$.

The excitation of charm basically interpolates between

$$\begin{aligned}
 C_{\text{GLS}}(\hat{a}_s, N_F = 3) &= 1 - \hat{a}_s - 3.58334\hat{a}_s^2 - 18.9757\hat{a}_s^3 - 160.444\hat{a}_s^4 \quad \text{and} \\
 C_{\text{GLS}}(\hat{a}_s, N_F = 4) &= 1 - \hat{a}_s - 3.25001\hat{a}_s^2 - 12.1975\hat{a}_s^3 - 82.9270\hat{a}_s^4. \tag{6.24}
 \end{aligned}$$

The charm corrections at lowest and first order (see Fig. 34) are given by

$$C_{\text{GLS}}^{\text{charm},(0)}(\xi) = \frac{\xi}{1 + \xi} \tag{6.25}$$

$$C_{\text{GLS}}^{\text{charm},(1)}(\xi) = C_F \left\{ -\frac{3\xi}{4(1 + \xi)} + \frac{3}{2} \frac{\ln(1 + \xi)}{1 + \xi} \right\}, \tag{6.26}$$

while at $O(a_s^2)$ the contributions to $L_{F_3,q}$ are given by

$$C_{\text{GLS}}^{\text{charm},(2)}(\xi) = \frac{1}{3} C_{\text{pBJ}}^{\text{charm},(2)}(\xi). \tag{6.27}$$

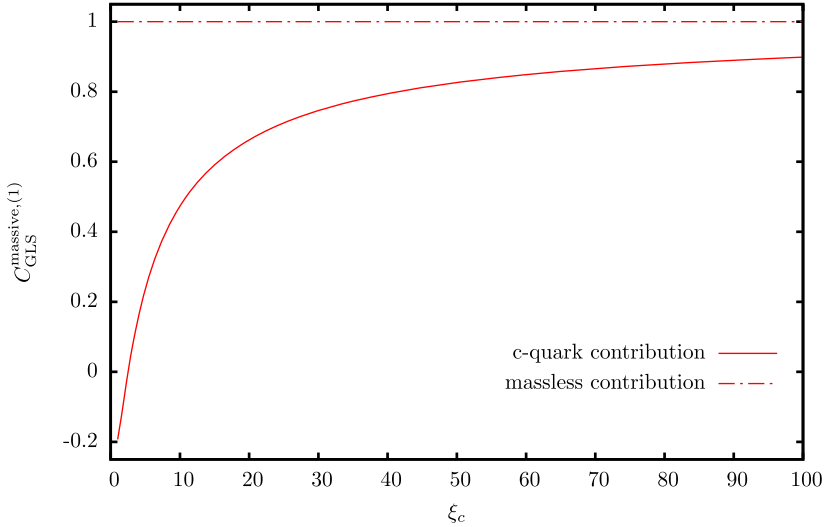


Fig. 34. The $O(a_s)$ coefficient $C_{\text{GLS}}^{\text{massive,(1)}}$ as a function of ξ_c , normalized to 1 in the limit $\xi \rightarrow \infty$.

Table 4

Comparison of C_{pBJ} in the massless approximation to $O(\hat{a}_s^4)$, $O(\hat{a}_s^2)$ for $N_F = 3$ massless flavors, and the $O(\hat{a}_s^2)$ contributions due to charm.

Q^2/GeV^2	$O(\hat{a}_s^4)$ massless	$O(\hat{a}_s^3)$ massless	Δ_{4-3}	Massive
30	0.9185	0.9207	-0.0022	0.0024
100	0.9324	0.9337	-0.0013	0.0013
10000	0.9588	0.9590	-0.0002	0.0004

The heavy flavor corrections up to $O(\hat{a}_s^2)$ are given by

$$C_{\text{GLS}}(\xi) = 1 + |V_{cd}|^2 \left[C_{\text{GLS}}^{\text{charm,(0)}}(\xi) - 1 \right] + \hat{a}_s \left\{ -1 + \frac{|V_{cd}|^2}{6} \left[C_{\text{GLS}}^{\text{charm,(1)}}(\xi) + 1 \right] \right\} + \hat{a}_s^2 \left\{ -\frac{55}{12} + \frac{1}{3} N_F + C_{\text{GLS}}^{\text{charm,(2)}}(\xi) \right\} + O(\hat{a}_s^3). \tag{6.28}$$

In Table 4 we compare the values of the Gross–Llewellyn Smith sum rule for different values of Q^2 to illustrate the effect of the heavy flavor contribution.

As in the case of the other sum rules, the charm corrections at $O(\hat{a}_s^2)$ turn out to be of the same size as the massless $O(\hat{a}_s^4)$ corrections.

6.5. The target mass corrections to the sum rules

For the target mass corrections it has been shown [66] that the correction factor to the massless structure function $F_2(N, Q^2)$ in Mellin space is given by

$$F_2^{\text{TM}}(N, Q^2) = \sum_{j=0}^{\infty} \left(\frac{M^2}{Q^2} \right)^j \binom{N+j}{j} \frac{N(N-1)}{(N+2j)(N+2j-1)} \frac{C_2^{N+2j} a_{N+2j}^{(2)}}{C_2^{1+2j} a_{1+2j}^{(2)}} \tag{6.29}$$

$$a_k^{(2)} = \int_0^1 dx x^{k-1} [u_v(x, Q^2) - d_v(x, Q^2)], \text{ with } a_1^{(2)} = 1 \tag{6.30}$$

$$C_2^k = \int_0^1 dx x^{k-1} C_2(x, Q^2), \quad C_2^1 = 1, \tag{6.31}$$

with M the nucleon mass, $(\Delta)a_{N+2j}^{(2)}$ the (non-perturbative) moments of the massless PDFs and C_2 the moments of the Wilson coefficient contributing to F_2 . Here we consider the flavor-non-singlet contribution $(F_2^{\bar{v}p} - F_2^{vp})/x$ which is relevant for the Adler-sum rule. Note that the first moment of C_2 , except for the tree-level contribution, vanishes, as has been proven to 3-loop order for the massless and massive Wilson coefficients (in the asymptotic region) by explicit calculations [14,72,78,89] and above for the massive contributions to the complete corrections at 2-loop order. One obtains

$$\lim_{N \rightarrow 1} F_2^{\text{TM}}(N, Q^2) = 0. \tag{6.32}$$

In contrast, the first moments of the structure functions F_1 and F_3 do not vanish at higher orders in QCD both in the massless and massive cases [1,90]. Moreover, both in the unpolarized [54, 65,90] and in the polarized cases, the target mass corrections are different for different structure functions, which are usually associated to other ones by current conservation, as in the case of $F_4(x, Q^2)$ and $F_5(x, Q^2)$.

In the case of the unpolarized Bjorken sum rule, the target mass correction factor is given by [1,90]

$$F_1^{\text{TM}}(N = 1, Q^2) = \sum_{j=0}^{\infty} \left(\frac{M^2}{Q^2}\right)^j (1+j) \frac{[C_1^{1+2j} + \frac{1}{1+2j} C_2^{1+2j}] a_{1+2j}}{C_1^1 a_1}. \tag{6.33}$$

Here $C_1^{(k)}$ denotes the k th moment of the Wilson coefficient contributing to the structure function $F_1^{\bar{v}p} - F_1^{vp}$.

The target mass corrections to the polarized Bjorken sum rule are given by [54,55]

$$g_1^{\text{TM}}(N = 1, Q^2) = \sum_{j=0}^{\infty} \left(\frac{M^2}{Q^2}\right)^j \frac{(1+j)}{(1+2j)^2} \frac{\Delta C_1^{1+2j} \Delta a_{1+2j}}{\Delta C_1^1 \Delta a_1} \tag{6.34}$$

$$\Delta a_k = \frac{1}{6} \int_0^1 dx x^{k-1} \left[\Delta u_v(x, Q^2) - \Delta d_v(x, Q^2) + 2 \left(\Delta \bar{u}(x, Q^2) - \Delta \bar{d}(x, Q^2) \right) \right] \tag{6.35}$$

$$\Delta C_1^k = \int_0^1 dx x^{k-1} \Delta C_1(x, Q^2), \tag{6.36}$$

where ΔC_1 is the polarized flavor-non-singlet Wilson coefficient corresponding to the structure function $g_1^{ep} - g_1^{en}$.

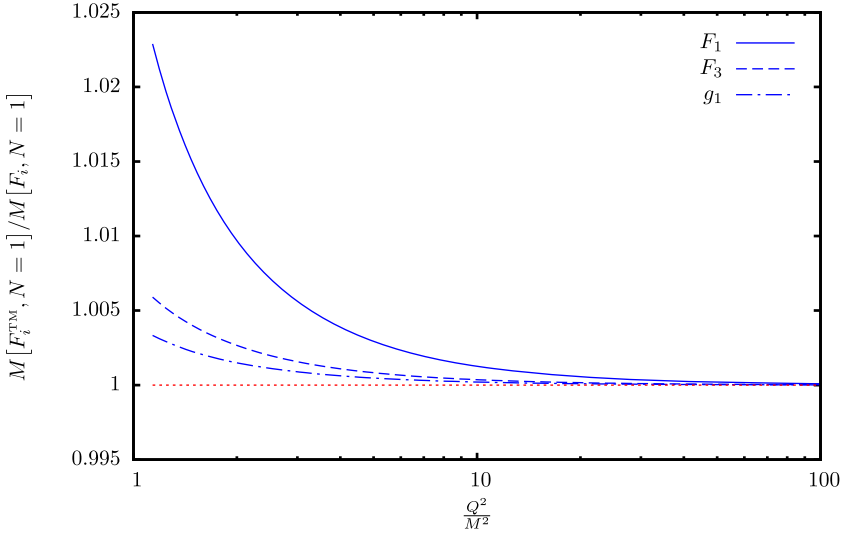


Fig. 35. The target mass corrections, normalized to the massless case, to the unpolarized (F_1) and polarized Bjorken sum rule (g_1) and the Gross–Llewellyn Smith sum rule (F_3).

For the target mass corrections to the Gross–Llewellyn Smith sum rule one obtains [1,90]

$$F_3^{\text{TM}}(N=1, Q^2) = \sum_{j=0}^{\infty} \left(\frac{M^2}{Q^2} \right)^j \frac{1+j}{1+2j} \frac{C_3^{1+2j} a_{1+2j}^{(3)}}{C_3^1 a_1^{(3)}}, \quad (6.37)$$

$$a_k^{(3)} = 2 \int_0^1 dx x^{k-1} \left[u_v(x, Q^2) + d_v(x, Q^2) \right], \quad \text{with } a_1^{(3)} = 6, \quad (6.38)$$

and C_3^k are the moments of the Wilson coefficient contributing to the flavor non-singlet combination $F_3^{\text{vp}} + F_3^{\text{pp}}$.

In Fig. 35 we illustrate the effect of the target mass corrections to the unpolarized and polarized Bjorken sum rule as well as the Gross–Llewellyn Smith sum rule, as a function of Q^2/M^2 , accounting only for the operator matrix elements $(\Delta)a_k^{(1,3)}$. We refer to the unpolarized PDFs [71] at NNLO and polarized PDFs [43] at NLO, and α_s at NNLO, to allow for a comparison of the different contributions up to NNLO.

The corrections diminish towards large virtualities Q^2 . At $Q^2 \sim 1 \text{ GeV}^2$ they amount +2.3%, 0.60% and 0.33% for the unpolarized Bjorken sum rule, the Gross–Llewellyn Smith sum rule and the polarized Bjorken sum rule, respectively.

7. Conclusions

We have calculated the complete heavy flavor corrections to the flavor non-singlet deep-inelastic structure functions $F_{1,2}$ and $g_{1,2}$ in the neutral current case, and to $F_{1,2}^{W^+-W^-}$ and $F_3^{W^++W^-}$ for charged current reactions. Here we considered the deep-inelastic region, which at least requests scales $Q^2 \gtrsim m_c^2$ or larger and $W^2 > 4 \text{ GeV}^2$. For the charged current non-

singlet combinations of structure functions also the Cabibbo suppressed Wilson coefficient $H_{i,q}$ contributes, which we have considered in the asymptotic region starting at $O(a_s^2)$ as an approximation. Since the deep-inelastic structure functions are inclusive observables, the formerly considered tagged flavor case [8,21] is not sufficient. We have accomplished the calculation for the inclusive case, to which at $O(a_s^2)$ also virtual corrections and real corrections with massless final states, containing massive virtual corrections, contribute. We present detailed numerical results for the different unpolarized and polarized structure functions for the charm and bottom contribution in the neutral current case and the charm contributions in the charged current case, which are the most important. We compared in all cases to the formerly calculated asymptotic corrections in the region $Q^2 \gg m^2$, showing that except for the structure function $F_2^{\text{NS}}(x, Q^2)$ this approximation holds only at higher scales, while for $F_2^{\text{nc,NS}}(x, Q^2)$ a very good agreement for $Q^2 \simeq 25 \text{ GeV}^2$ is obtained in the case of charm. In those cases in which the asymptotic 3-loops corrections are available, we have partly compared to these corrections as well. The $O(a_s^2)$ non-singlet heavy flavor effects are of the order of several per cent of the whole non-singlet structure function and are of relevance in precision measurements reaching this accuracy. The corrections will become even more important in the case of planned high-luminosity measurements at facilities like the EIC [91], future neutrino factories [92] or the LHeC [93].

We also investigated the heavy flavor corrections for deep-inelastic scattering sum rules, such as the Adler, polarized Bjorken, unpolarized Bjorken and Gross–Llewellyn Smith sum rule. While the corrections vanish in case of the Adler sum rule, finite corrections are obtained to the other three sum rules. They turn out to be of the same size as the massless $O(a_s^4)$ corrections which have been calculated recently and complete the picture from the side of the heavy quarks. Here it is important to refer to the inclusive rather than to the tagged heavy flavor case, since in the latter, logarithmic terms in the region of larger Q^2 would remain, after having already performed the renormalization completely (e.g. in the $\overline{\text{MS}}$ scheme) [10]. In the inclusive case, on the other hand, the transition from $N_F \rightarrow N_F + 1$ proceeds smoothly. We also quantified the effect of target mass corrections to the deep inelastic sum rules. In general it turns out that for the sum rules the transition $N_F \rightarrow N_F + 1$ proceeds slowly in $\xi = Q^2/m^2$. Therefore assuming scale matching at $Q^2 = m^2$ is, at least here, not appropriate.

Acknowledgements

We would like to thank A. Behring, K. Chetyrkin, C. Schneider, and A. Vogt for discussions. The graphs have been drawn using AxoDraw [101]. This work was supported in part by the European Commission through contract PITN-GA-2012-316704 (HIGGSTOOLS).

Appendix A. Calculation of the Compton contribution to $g_1^{\text{NS},(2)}$

In this appendix we calculate the contribution of the subprocess

$$q(p_1) + \gamma^*(q) \longrightarrow q(p_2) + Q(p_c) + \overline{Q}(p_{\overline{c}}) \tag{A.1}$$

to the non-singlet coefficient function $L_{g_1,q}^{\text{NS},(2)}$, which is given by Compton scattering diagrams shown in Fig. 1. The structure function $g_1(z)$ is extracted from the antisymmetric part of the hadronic tensor $W^{\mu\nu}$, given by

$$\widehat{W}_A^{\mu\nu}(p, q, s) = -\frac{m_0}{2p \cdot q} \epsilon^{\mu\nu\alpha\beta} q_\alpha \left[\widehat{g}_{1,0}(z, Q^2) s_\beta + \widehat{g}_{2,0}(z, Q^2) \left(s_\beta - \frac{q \cdot s}{q \cdot p} p_\beta \right) \right], \tag{A.2}$$

where $z = \frac{Q^2}{2p \cdot q}$ and m_0 , p and s are the mass, momentum and spin of the incoming light quark, with

$$p \cdot s = 0, \quad s \cdot s = -1. \quad (\text{A.3})$$

Later on we will consider the limit $m_0 \rightarrow 0$. The term $\widehat{g}_{1,0}(z, Q^2)$ can be obtained by [41]

$$\widehat{g}_{1,0}(z, Q^2) = \frac{2}{(d-2)(d-3)} \frac{1}{p \cdot q} \epsilon_{\mu\nu\rho\sigma} p^\rho q^\sigma \widehat{W}_A^{\mu\nu} \left(z, q, s = \frac{p}{m_0} \right). \quad (\text{A.4})$$

The hadronic tensor is given by

$$\begin{aligned} \widehat{W}_A^{\mu\nu} &= 4\pi \alpha_s^2 C_F T_F \int \frac{d^d p_2}{(2\pi)^d} \frac{d^d p_c}{(2\pi)^d} \frac{d^d p_{\bar{c}}}{(2\pi)^d} (2\pi)^d \delta^d(p+q-p_2-p_c-p_{\bar{c}}) \\ &\quad \left\{ \text{Tr} \left[\frac{\gamma_5 \not{s}}{2} (\not{p} + m_0) \left(\frac{\gamma^\nu (\not{p} + \not{q} + m_0) \gamma_\sigma (\not{p}_2 + m_0) \gamma_\rho (\not{p} + \not{q} + m_0) \gamma^\mu}{[(p+q)^2 - m_0^2]^2} \right. \right. \right. \\ &\quad + \frac{\gamma^\nu (\not{p} + \not{q} + m_0) \gamma_\sigma (\not{p}_2 + m_0) \gamma^\mu (\not{p}_2 - \not{q} + m_0) \gamma_\rho}{[(p+q)^2 - m_0^2][(p_2 - q)^2 - m_0^2]} \\ &\quad + \frac{\gamma_\sigma (\not{p}_2 - \not{q} + m_0) \gamma^\nu (\not{p}_2 + m_0) \gamma_\rho (\not{p} + \not{q} + m_0) \gamma^\mu}{[(p+q)^2 - m_0^2][(p_2 - q)^2 - m_0^2]} \\ &\quad \left. \left. \left. + \frac{\gamma_\sigma (\not{p}_2 - \not{q} + m_0) \gamma^\nu (\not{p}_2 + m_0) \gamma^\mu (\not{p}_2 - \not{q} + m_0) \gamma_\rho}{[(p_2 - q)^2 - m_0^2]^2} \right) \right] \right\} \\ &\quad \times \frac{4}{[q_2^2]^2} \left[p_c^\rho p_{\bar{c}}^\sigma + p_c^\sigma p_{\bar{c}}^\rho - (p_c \cdot p_{\bar{c}} + m^2) g^{\rho\sigma} \right] \\ &\quad \times (2\pi)^3 \delta_+(p_2^2 - m_0^2) \delta_+(p_c^2 - m^2) \delta_+(p_{\bar{c}}^2 - m^2) \\ &\equiv 4\pi \alpha_s^2 C_F T_F \int \frac{d^d p_2}{(2\pi)^d} \frac{d^d p_c}{(2\pi)^d} \frac{d^d p_{\bar{c}}}{(2\pi)^d} (2\pi)^d \delta^d(p+q-p_2-p_c-p_{\bar{c}}) \\ &\quad \times (2\pi)^3 \delta_+(p_2^2 - m_0^2) \delta_+(p_c^2 - m^2) \delta_+(p_{\bar{c}}^2 - m^2) \mathcal{T}_{\rho\sigma}^{\mu\nu}(p_2, q_2) J_c^{\rho\sigma}(p_c, p_{\bar{c}}), \end{aligned} \quad (\text{A.5})$$

where m , $(p_{\bar{c}})$ p_c are the mass and four momenta of the heavy (anti-)quark, $q_2 = p_c + p_{\bar{c}}$ and p_2 denotes the momentum of the light quark in the final state. The distribution δ_+ is defined by

$$\delta_+(p^2 - m^2) = \delta(p^2 - m^2) \theta(p^0). \quad (\text{A.6})$$

The last line of Eq. (A.5) emphasizes that the phase space integral is factorized. The tensors $\mathcal{T}_{\rho\sigma}^{\mu\nu}$ and $J_c^{\rho\sigma}$ read

$$\begin{aligned} \mathcal{T}_{\rho\sigma}^{\mu\nu} &= \frac{1}{[q_2^2]^2} \left\{ \text{Tr} \left[\frac{\gamma_5 \not{s}}{2} (\not{p} + m_0) \left(\frac{\gamma^\nu (\not{p} + \not{q} + m_0) \gamma_\sigma (\not{p}_2 + m_0) \gamma_\rho (\not{p} + \not{q} + m_0) \gamma^\mu}{[(p+q)^2 - m_0^2]^2} \right. \right. \right. \\ &\quad + \frac{\gamma^\nu (\not{p} + \not{q} + m_0) \gamma_\sigma (\not{p}_2 + m_0) \gamma^\mu (\not{p}_2 - \not{q} + m_0) \gamma_\rho}{[(p+q)^2 - m_0^2][(p_2 - q)^2 - m_0^2]} \\ &\quad + \frac{\gamma_\sigma (\not{p}_2 - \not{q} + m_0) \gamma^\nu (\not{p}_2 + m_0) \gamma_\rho (\not{p} + \not{q} + m_0) \gamma^\mu}{[(p+q)^2 - m_0^2][(p_2 - q)^2 - m_0^2]} \\ &\quad \left. \left. \left. + \frac{\gamma_\sigma (\not{p}_2 - \not{q} + m_0) \gamma^\nu (\not{p}_2 + m_0) \gamma^\mu (\not{p}_2 - \not{q} + m_0) \gamma_\rho}{[(p_2 - q)^2 - m_0^2]^2} \right) \right] \right\}, \\ J_c^{\rho\sigma} &= 4 \left[p_c^\rho p_{\bar{c}}^\sigma + p_c^\sigma p_{\bar{c}}^\rho - (p_c \cdot p_{\bar{c}} + m^2) g^{\rho\sigma} \right]. \end{aligned} \quad (\text{A.7})$$

We consider the incoming quark directed in the \widehat{z} axis. The momentum and spin of a longitudinally polarized quark are then given by

$$\begin{aligned}
 p &= (\sqrt{p^2 + m_0^2}, 0, 0, p) \longrightarrow p(1, 0, 0, 1) + \left(\frac{m_0^2}{2p}, \vec{0} \right), \\
 s &= \frac{1}{m_0}(p, 0, 0, \sqrt{p^2 + m_0^2}) \longrightarrow \frac{p}{m_0}(1, 0, 0, 1) + \left(0, 0, 0, \frac{m_0}{2p} \right), \quad \text{for } m_0 \rightarrow 0.
 \end{aligned}
 \tag{A.8}$$

Therefore, it is important to retain the linear terms in the mass m_0 , which is finally canceled by the normalization of the spin vector.

The integrals are finite in $d = 4$ dimensions to which we turn from now on. The phase space integrals can be carried out analytically leading to

$$\begin{aligned}
 \widehat{g}_{1,0}(z, Q^2) &= -\frac{g_s^4 C_F T_F}{12\pi^3} \int_{4m^2}^{Q^2 \left(\frac{1-z}{z}\right)} \frac{d\mu^2}{(2\pi)} \sqrt{\frac{\mu^2 - 4m^2}{\mu^2}} \left[\frac{\mu^2 + 2m^2}{2} \right] \frac{Q^2(1-z) - z\mu^2}{8Q^4(1-z)\mu^4} \\
 &\times \left\{ \frac{2}{(1-z)^2(z\mu^2 - Q^2)} \left[\mu^4 z^2(4z^2 - 6z + 3) \right. \right. \\
 &\quad \left. \left. + \mu^2 Q^2 z(-8z^3 + 14z^2 - 9z + 2) + 3Q^4(2z^3 - 4z^2 + 3z - 1) \right] \right. \\
 &\quad \left. + 4 \frac{2\mu^4 z^3 - 2\mu^2 Q^2 z(2z^2 - z + 1) + Q^4(1 + z^2)}{(Q^2(1-z) - \mu^2 z)} \right. \\
 &\quad \left. \times \ln \left(\frac{\mu^2 z^2}{(1-z)(Q^2 - z\mu^2)} \right) \right\}.
 \end{aligned}
 \tag{A.9}$$

It is convenient to perform the μ^2 -integral over

$$\beta = \sqrt{1 - \frac{4m^2}{\mu^2}}.
 \tag{A.10}$$

After applying this transformation, the integral becomes

$$\begin{aligned}
 \widehat{g}_{1,0}(z, Q^2) &= \frac{4a_s^2 C_F T_F}{3} \int_0^{\sqrt{1 - \frac{4z}{\xi(1-z)}}} d\beta \frac{\beta^2(\beta^2 - 3)}{(1 - \beta^2)^3 \xi^3(1-z)^3 \left(\beta^2 - 1 + \frac{4z}{\xi}\right)} \\
 &\left\{ \left[16(1 - \beta^2)\xi(4(z-1)z^2 + 1)z^2 - 64(4z^2 - 6z + 3)z^3 \right. \right. \\
 &\quad \left. \left. - 3(1 - \beta^2)^3 \xi^3(z-1)^2(2(z-1)z + 1) + 4(1 - \beta^2)^2 \xi^2(z-1) \right] \right. \\
 &\quad \times (z(4z(2z-5) + 15) - 5)z \left. \right] + 2(1-z)^2(\beta^2 - 1 + \frac{4z}{\xi})\xi \left[32z^3 \right. \\
 &\quad \left. \left. - 8z(1-z+2z^2)\xi(1 - \beta^2) + (1+z^2)\xi^2(1 - \beta^2)^2 \right] \ln \left(\frac{\frac{4z}{\xi(1-z)} - \frac{4z}{\xi}}{1 - \frac{4z}{\xi} - \beta^2} \right) \right\}.
 \end{aligned}
 \tag{A.11}$$

This term can finally be integrated analytically to yield (3.9).

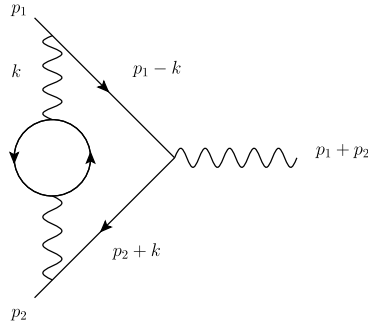


Fig. 36. Two-loop diagrams with vacuum polarization insertions.

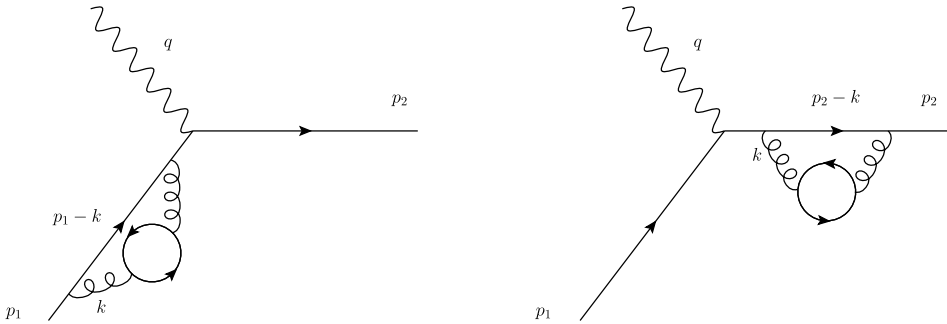


Fig. 37. Reducible diagrams with fermion self energy insertion.

Appendix B. The virtual corrections

The interaction of an on-shell fermion and the electromagnetic current is parameterized in terms of the Dirac and Pauli form factors $F_1(q^2)$, $F_2(q^2)$, respectively. In the space-like case one has

$$\langle p_2 | J^\mu(q^2) | p_1 \rangle = \bar{u}(p_2) \Gamma^\mu u(p_1) = \bar{u}(p_2) \left[\gamma^\mu F_1(q^2) - \frac{F_2(q^2)}{4m_0} \sigma^{\mu\nu} q_\nu \right] u(p_1), \quad (B.1)$$

where $\sigma^{\mu\nu} = \frac{i}{2}[\gamma^\mu, \gamma^\nu]$. The correction can be obtained by the subtracted dispersion relation for the Dirac form factor.

We will first perform the calculation in the time-like case and obtain then the space-like result by analytic continuation. One has

$$F_1(s) - F_1(0) = \frac{s}{\pi} \int_0^\infty dz \frac{\text{Im}(F_1(z))}{z(z-s)}, \quad (B.2)$$

which can be calculated from the diagrams in Figs. 36, 37 and applying the Ward identity of Subsection B.1, with $s = (p_1 + p_2)^2$.

Note that the integral (B.2) in the case of the unsubtracted dispersion relation diverges. The calculation proceeds in a similar way as in Refs. [94,95]. We will initially work in d dimensions and use quarks of mass m_0 for the external particles and m for the heavy quark in the loop. Later on we take the limit $d = 4$ and $m_0 = 0$.

The Dirac form factor is projected to

$$F_1(s) = -\frac{1}{2(d-2)(s-4m_0^2)} \times \text{Tr} \left[\left(\gamma^\mu + \frac{2m_0(d-1)}{s-4m_0^2} (p_1 - p_2)^\mu \right) (\not{p}_2 - m_0) \Gamma^\mu (\not{p}_1 + m_0) \right]. \tag{B.3}$$

The contribution of the diagram in Fig. 36 to the vertex Γ^μ is given by

$$\begin{aligned} & \bar{v}(p_2) \Gamma^\mu u(p_1) \\ &= C_F T_F \int \left\{ \frac{\bar{v}(p_2) (i g_s \gamma^\rho) (-i) (\not{p}_2 + \not{k} - m) \gamma^\mu i (\not{p}_1 - \not{k} + m) (i g_s \gamma^\sigma) u(p_1)}{[(p_2 + k)^2 - m_0^2 + i0][(p_1 - k)^2 - m_0^2 + i0]} \right. \\ & \quad \left. \times \left(\frac{-i}{k^2 + i0} \right)^2 i \Pi(k^2) (k^2 g_{\rho\sigma} - k_\rho k_\sigma) \right\} \frac{d^d k}{(2\pi)^d}, \end{aligned} \tag{B.4}$$

where $\Pi(k^2)$ denotes the vacuum polarization

$$\Pi(k^2) - \Pi(0) = -\frac{\alpha_s}{\pi} \frac{k^2}{3} \int_{4m^2}^{\infty} \frac{dx}{x^2} \frac{(x+2m^2)}{x-k^2} \sqrt{1 - \frac{4m^2}{x}} \tag{B.5}$$

leading to

$$\begin{aligned} F_1(s) = & -i \frac{g_s^2 C_F T_F}{2(d-2)(s-4m_0^2)} \int \frac{d^d k}{(2\pi)^d} \left\{ \text{Tr} \left[\left(\gamma^\mu + \frac{2m(d-1)}{s-4m^2} (p_1 - p_2)^\mu \right) \right. \right. \\ & \left. \left. \times (\not{p}_2 - m_0) \gamma^\rho (\not{p}_2 + \not{k} - m_0) \gamma_\mu (\not{p}_1 - \not{k} + m_0) \gamma^\sigma (\not{p}_1 + m_0) \right] \right. \\ & \left. \times \frac{(k^2 g_{\rho\sigma} - k_\rho k_\sigma) \Pi(k^2)}{[k^2 + i0]^2 [(p_1 - k)^2 - m_0^2 + i0][(p_2 + k)^2 - m_0^2 + i0]} \right\}. \end{aligned} \tag{B.6}$$

Its imaginary part is found putting the propagators

$$\begin{aligned} \frac{1}{[(p_1 - k)^2 - m_0^2 + i0]} & \rightarrow -(2\pi i) \delta_+((p_1 - k)^2 - m_0^2), \\ \frac{1}{[(p_2 + k)^2 - m_0^2 + i0]} & \rightarrow -(2\pi i) \delta_+((p_2 + k)^2 - m_0^2), \end{aligned} \tag{B.7}$$

on shell, cf. [94,95]. Note that when taking the cut a minus sign has to be introduced [96,97]

$$\begin{aligned} 2\text{Im}(F_1(s)) = & \frac{g_s^2 C_F T_F}{2(d-2)(s-4m_0^2)} \int \left\{ \text{Tr} \left[\left(\gamma^\mu + \frac{2m(d-1)}{s-4m_0^2} (p_1 - p_2)^\mu \right) \right. \right. \\ & \left. \left. \times (\not{p}_2 - m_0) \gamma^\rho (\not{p}_2 + \not{k} - m_0) \gamma_\mu (\not{p}_1 - \not{k} + m_0) \gamma^\sigma (\not{p}_1 + m_0) \right] \right. \\ & \left. \times \frac{(k^2 g_{\rho\sigma} - k_\rho k_\sigma) \Pi(k^2)}{[k^2 + i0]^2} \right\} \\ & \times (2\pi)^2 \delta_+((p_1 - k)^2 - m_0^2) \delta_+((p_2 + k)^2 - m_0^2) \frac{d^d k}{(2\pi)^d}. \end{aligned} \tag{B.8}$$

The longitudinal parts of the photon polarization can be shown to vanish. One finally obtains

$$\begin{aligned} & \text{Im}(F_1(s)) \\ &= \frac{\alpha_s^2}{6} C_F T_F \frac{1}{\sqrt{s}} \left(\frac{s}{4} - m_0^2\right)^{\frac{d-3}{2}} \frac{\Omega_{d-3}}{(2\pi)^{d-2}} \int_{4m^2}^{\infty} \frac{dx^2}{x^2} \sqrt{1 - \frac{4m^2}{x}} (x + 2m^2) \\ & \quad \times \int_0^\pi d\theta (\sin\theta)^{d-3} \frac{\cos^2\theta(s + 4m_0^2(d-2)) + \cos\theta(s(6-d) - 4dm_0^2) + s(d-3)}{(s - 4m_0^2)(1 - \cos\theta) + 2x}, \end{aligned} \tag{B.9}$$

with [98]

$$\Omega_d = \frac{2\pi^{\frac{d+1}{2}}}{\Gamma\left(\frac{d+1}{2}\right)}. \tag{B.10}$$

We are now turning to $d = 4$ and obtain

$$\begin{aligned} \text{Im}(F_1(s)) &= -\frac{\alpha_s^2}{24\pi} C_F T_F \sqrt{1 - \xi_1} \int_0^\pi d\theta \sin\theta [\cos^2\theta(1 + 2\xi_1) + 2\cos\theta(1 - 2\xi_1) + 1] \\ & \quad \times \int_0^1 d\beta \frac{\beta^2(\beta^2 - 3)}{(1 - \cos\theta)(1 - \xi_1) + 2\xi_2 - \beta^2(1 - \xi_1)(1 - \cos\theta)}, \end{aligned} \tag{B.11}$$

with

$$\xi_2 = \frac{4m^2}{s}. \tag{B.12}$$

Furthermore we consider the limit $\frac{4m_0^2}{s} = \xi_1 \rightarrow 0$. After integrating over β we have

$$\begin{aligned} \text{Im}(F_1(s, m_0 = 0)) &= -\frac{\alpha_s^2}{24\pi} \int_{-1}^1 dX \frac{(1 + X)^2}{(1 - X)^2} \left[\frac{5 - 5X - 6\xi_2}{3} \right. \\ & \quad \left. - \sqrt{1 + \frac{2\xi_2}{1 - X}} (1 - X - \xi_2) \ln \left(\frac{\sqrt{1 + \frac{2\xi_2}{1 - X}} + 1}{\sqrt{1 + \frac{2\xi_2}{1 - X}} - 1} \right) \right], \end{aligned} \tag{B.13}$$

where $X = \cos\theta$. Trading the root in (B.13) as a new integration variable one obtains

$$\begin{aligned} & \text{Im}(F_1(s, m_0 = 0)) \\ &= -\frac{\alpha_s^2}{24\pi} \left[-\frac{5}{9}(53 + 33\xi_2) + \frac{1}{3}\sqrt{1 + \xi_2}(38 + 23\xi_2) \ln \left(\frac{\sqrt{1 + \xi_2} + 1}{\sqrt{1 + \xi_2} - 1} \right) \right. \\ & \quad \left. + \left(-2 + \frac{3\xi_2^2}{4} \right) \ln^2 \left(\frac{\sqrt{1 + \xi_2} + 1}{\sqrt{1 + \xi_2} - 1} \right) \right]. \end{aligned} \tag{B.14}$$

In order to determine the complete expression of the form factor in the time-like region, we use again the subtracted relation (B.2)

$$\begin{aligned}
 F_1(s, m_0 = 0) &= -\frac{\alpha_s^2}{24\pi^2} \left\{ -\frac{1213}{54} - \frac{119}{3} s_\xi^2 + \left(\frac{200}{9} + \frac{110s_\xi^2}{3} \right) \ln(2) \right. \\
 &\quad - \frac{5}{9} (20 + 33s_\xi^2) \ln(1 - s_\xi^2) - s_\xi \frac{15 + 23s_\xi^2}{3} \left[\text{Li}_2 \left(-\frac{1 - s_\xi}{1 + s_\xi} \right) - \text{Li}_2 \left(-\frac{1 + s_\xi}{1 - s_\xi} \right) \right] \\
 &\quad \left. - \left(\frac{5}{2} + 3s_\xi^2 - \frac{3s_\xi^4}{2} \right) \left[\text{Li}_3 \left(-\frac{1 - s_\xi}{1 + s_\xi} \right) + \text{Li}_3 \left(-\frac{1 + s_\xi}{1 - s_\xi} \right) - 2\zeta_3 \right] \right\}, \tag{B.15}
 \end{aligned}$$

where

$$s_\xi = \sqrt{1 + \xi_2}. \tag{B.16}$$

The analytic continuation of (B.15) to the space-like region is obtained by replacing

$$s_\xi \rightarrow \hat{s}_\xi = \sqrt{1 - \frac{4m^2}{Q^2}} \equiv \tilde{\lambda}, \tag{B.17}$$

cf. Eq. (3.12). The real part of Eq. (B.15), if considered in the time-like region, may be compared with a result in [99], Eq. (A1), for the Drell–Yan process and agrees.

B.1. A Ward identity

In the following we derive the relation of the self-energy insertions to $F_1(0)$ through a Ward identity. The graphs of Fig. 37 obey

$$\frac{1}{2} \left[(a) + (b) \right] = (Z_2 - 1) \bar{u}(p_2) (-ie \gamma_\mu) u(p_1), \tag{B.18}$$

where e denotes the electric charge.

By following the notation of [100], we define $-i\Sigma(p^2)$ as the proper self energy diagram in Fig. 38 and we find the renormalization constant by taking the residue of the complete quark propagator on the mass shell. In the case of massless external fermions we have

$$iS_F = \frac{i}{\not{p} - \Sigma(p)} \xrightarrow{p^2 \rightarrow 0} i \frac{Z_2}{\not{p}}, \tag{B.19}$$

so that $Z_2 = 1 + \frac{\Sigma(p^2)\not{p}}{p^2}$ at leading order. The next step is to extract the spin structure of the self energy $\Sigma(p^2) = \not{p} \bar{\Sigma}(p^2)$, where the latter object is a scalar function, so that we can write the renormalization constant Z_2 as

$$Z_2 = 1 + \bar{\Sigma}(p). \tag{B.20}$$

By introducing (B.20) into Eq. (B.18), we obtain the contribution of self energy diagrams.

We consider the derivative of the self energy

$$-i\Sigma(p^2) = -ig_s^4 C_F T_F \int \frac{d^d k}{(2\pi)^d} \frac{\gamma^\alpha (\not{p} - \not{k}) \gamma^\beta}{(p - k)^2 (k^2)^2} \left[k^2 g_{\alpha\beta} - k_\alpha k_\beta \right] \Pi(k^2), \tag{B.21}$$

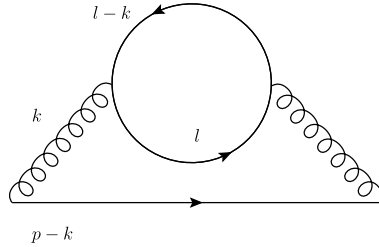


Fig. 38. Proper self energy diagram.

with $\Pi(k^2)$ given in Eq. (B.5). It reads

$$\begin{aligned} \frac{\partial \Sigma}{\partial p_\mu} &= g_s^4 C_F T_F \int \frac{d^d k}{(2\pi)^d} \Pi(k^2) \left[k^2 g_{\alpha\beta} - k_\alpha k_\beta \right] \\ &\quad \times \left\{ \frac{\gamma^\alpha \gamma_\mu \gamma^\beta}{(p-k)^2 [k^2]^2} - 2(p-k)_\mu \frac{\gamma^\alpha (\not{p}-\not{k}) \gamma^\beta}{[(p-k)^2]^2 [k^2]^2} \right\} \\ &= g_s^4 C_F T_F \int \frac{d^d k}{(2\pi)^d} \Pi(k^2) \left[k^2 g_{\alpha\beta} - k_\alpha k_\beta \right] \left\{ - \frac{\gamma^\alpha (\not{p}-\not{k}) \gamma_\mu (\not{p}-\not{k}) \gamma^\beta}{[(p-k)^2]^2 [k^2]^2} \right\}. \end{aligned} \tag{B.22}$$

The vertex function is given by

$$\begin{aligned} -ie \Lambda_\mu(p_2, p_1) &\equiv -ie F_1(q^2) \gamma_\mu = (-ie) g_s^4 C_F T_F \int \frac{d^d k}{(2\pi)^d} \Pi(k^2) \left[k^2 g_{\alpha\beta} - k_\alpha k_\beta \right] \\ &\quad \times \left\{ \frac{\gamma^\alpha (\not{p}_2 - \not{k}) \gamma_\mu (\not{p}_1 - \not{k}) \gamma^\beta}{[(p_2 - k)^2][(p_1 - k)^2][k^2]^2} \right\}, \end{aligned} \tag{B.23}$$

with $(p_2 - p_1)^2 = q^2$. In the limit of zero momentum transfer, $q^2 \rightarrow 0$, the vertex function becomes $\Lambda_\mu(0) = F_1(0) \gamma_\mu$. By comparing (B.23) and (B.22) one gets

$$\begin{aligned} \Lambda_\mu(0) &\rightarrow g_s^4 C_F T_F \int \frac{d^d k}{(2\pi)^d} \Pi(k^2) \left[k^2 g_{\alpha\beta} - k_\alpha k_\beta \right] \left\{ \frac{\gamma^\alpha (\not{p} - \not{k}) \gamma_\mu (\not{p} - \not{k}) \gamma^\beta}{[(p-k)^2]^2 [k^2]^2} \right\} \\ &= - \frac{\partial \Sigma(p^2)}{\partial p^\mu}, \end{aligned} \tag{B.24}$$

i.e.

$$F_1(Q^2 = 0) \gamma_\mu = -\gamma_\mu \bar{\Sigma}(p) - \not{p} \frac{\partial \bar{\Sigma}}{\partial p^\mu}. \tag{B.25}$$

Eq. (B.25) allows to write the function $\bar{\Sigma}(p)$ in terms of the form factor at zero momentum transfer. Therefore (B.18) can be written as

$$\begin{aligned} \frac{1}{2} \left[(a) + (b) \right] &= \left[\frac{1}{2} \bar{\Sigma}(p_1) + \frac{1}{2} \bar{\Sigma}(p_2) \right] \bar{u}(p_2) (-ie \gamma_\mu) u(p_1) \\ &= \frac{1}{2} \bar{u}(p_2) \left(-ie \bar{\Sigma}(p_1) \gamma_\mu \right) u(p_1) + \frac{1}{2} \bar{u}(p_2) \left(-ie \bar{\Sigma}(p_2) \gamma_\mu \right) u(p_1) \\ &= \frac{1}{2} \bar{u}(p_2) \left[-ie \left(-F_1(0) \gamma_\mu - \not{p}_1 \frac{\partial \bar{\Sigma}(p_1)}{\partial p_1^\mu} \right) \right] u(p_1) \end{aligned}$$

$$+ \frac{1}{2} \bar{u}(p_2) \left[-ie \left(-F_1(0)\gamma_\mu - \not{p}_2 \frac{\partial \bar{\Sigma}(p_2)}{\partial p_2^\mu} \right) \right] u(p_1), \tag{B.26}$$

where in the last identity we introduced $\bar{\Sigma}(p_i)$ in terms of $F_1(0)$, according to the relation (B.25). In the expression above, all the terms proportional to $\frac{\partial \bar{\Sigma}(p)}{\partial p^\mu}$ vanish because of the Dirac equation, finally

$$\frac{1}{2} \left[(a) + (b) \right] = \bar{u}(p_2) \left(ie F_1(0)\gamma_\mu \right) u(p_1). \tag{B.27}$$

In conclusion, the scattering amplitude of a massless quark and an off shell photon with momentum q is given by the sum of the virtual correction to the proper qq -gauge boson vertex, depicted in Fig. 36, which we computed via dispersion relations up to an offset $F_1(0)$, and the self energies contributions above, which proves that the results of the subtracted dispersive approach Eqs. (B.15), (B.2) give the complete renormalized form factor.

Appendix C. The first moment

In the following we derive the heavy flavor contributions to the Bjorken sum rule to $O(a_s^2)$. The Compton contribution is obtained by the integral

$$A_{g_1}(\xi) = \int_0^{\frac{\xi}{\xi+4}} dz \widehat{g}_1(z, Q^2), \tag{C.1}$$

where $\widehat{g}_1(z, Q^2)$ is given by the integral (A.11), see also (3.9). To obtain the analytic expression, it is easier to step back one integral and to use

$$A_{g_1}(\xi) = \int_0^{\frac{\xi}{\xi+4}} dz \int_{4m^2}^{Q^2 \left(\frac{1-z}{z}\right)} I(z, \mu^2) d\mu^2 = \int_{4m^2}^{\infty} d\mu^2 \int_0^{\frac{Q^2}{Q^2+\mu^2}} I(z, \mu^2) dz, \tag{C.2}$$

where the integrand $I(z, \mu^2)$ is the same (including normalization) as in (A.9). The z -integral yields

$$\begin{aligned} A_{g_1}(Q^2) = & \hat{a}_s^2 C_F T_F \int_1^\infty dx \sqrt{\frac{x-1}{x}} \frac{1+2x}{1152\xi^2 x^4} \left\{ 4x\xi^3 - 1088x^3\xi + 248x^2\xi^2 \right. \\ & + 192x^2(\xi - 4x)^2 \ln^2\left(\frac{4x}{\xi}\right) - \left(1280x^4 + 512x^3\xi - 16x\xi^3 - \xi^4 \right) \ln(\xi) \\ & - 32x^2 \ln\left(\frac{4x}{\xi}\right) \left[40x^2 + 40x\xi - 9\xi^2 + 6(\xi - 4x)^2 \ln\left(\frac{4x - \xi}{\xi}\right) \right] \\ & + \left[1280x^4 + 512x^3\xi - 16x\xi^3 - \xi^4 \right] \ln(\xi + 4x) \\ & \left. + 192x^2(\xi - 4x)^2 \text{Li}_2\left(\frac{\xi}{4x}\right) \right\}, \tag{C.3} \end{aligned}$$

where $x = \mu^2/(4m^2)$. The result of the last integration can be conveniently expressed in terms of the variables

$$\lambda = \sqrt{1 + \frac{4}{\xi}}, \quad \tilde{\lambda} = \sqrt{1 - \frac{4}{\xi}}. \quad (\text{C.4})$$

The x -integral results into

$$\begin{aligned} A_{g_1}(\xi) = & \hat{a}_s^2 C_F T_F \left\{ \left(\frac{2}{\xi^2} - \frac{1}{3} \right) \left[\text{Li}_3 \left(\frac{\tilde{\lambda} + 1}{\tilde{\lambda} - 1} \right) + \text{Li}_3 \left(\frac{\tilde{\lambda} - 1}{\tilde{\lambda} + 1} \right) - 2\zeta_3 \right] \right. \\ & + \tilde{\lambda} \left(\frac{19}{18} - \frac{23}{9\xi} \right) \left[\text{Li}_2 \left(\frac{\tilde{\lambda} + 1}{\tilde{\lambda} - 1} \right) - \text{Li}_2 \left(\frac{\tilde{\lambda} - 1}{\tilde{\lambda} + 1} \right) \right] - \frac{5}{12\xi^2} \ln^2 \left(\frac{\lambda + 1}{\lambda - 1} \right) \\ & + \lambda \ln \left(\frac{\lambda + 1}{\lambda - 1} \right) \left[-\frac{527}{2520} - \frac{401}{420\xi} - \frac{53\xi}{2520} - \frac{\xi^2}{1680} \right] \\ & \left. + \ln(\xi) \left[\frac{265}{108} - \frac{55}{9\xi} + \frac{\xi}{45} + \frac{\xi^2}{1680} \right] + \frac{19591}{1260\xi} + \frac{\xi}{840} - \frac{42047}{9072} \right\} \end{aligned} \quad (\text{C.5})$$

We have still to add the virtual contribution (3.12) and the contribution due to the term with massless final states (3.11) which yields

$$\begin{aligned} A_{g_1}(\xi) = & \hat{a}_s^2 C_F T_F \left\{ -\frac{5}{12\xi^2} \ln^2 \left(\frac{\lambda + 1}{\lambda - 1} \right) - \frac{\lambda(3\xi^3 + 106\xi^2 + 1054\xi + 4812)}{5040\xi} \right. \\ & \left. \times \ln \left(\frac{\lambda + 1}{\lambda - 1} \right) + \frac{6\xi^2 + 2735\xi + 11724}{5040\xi} + \frac{\xi(3\xi + 112)}{5040} \ln(\xi) + \frac{1}{4} \ln(\xi) \right\}. \end{aligned} \quad (\text{C.6})$$

In the asymptotic limit one obtains

$$A_{g_1}(\xi) \propto \hat{a}_s^2 C_F T_F \frac{1}{2} + O \left(\frac{\ln^2(\xi)}{\xi} \right). \quad (\text{C.7})$$

Note that the pure Compton contribution diverges like $\sim \ln^3(\xi)$. Adding the virtual corrections, the term still diverges $\sim \ln(\xi)$. This behavior is obtained considering tagged heavy quark production instead of the inclusive heavy flavor corrections, cf. [27].

References

- [1] J. Blümlein, *Prog. Part. Nucl. Phys.* **69** (2013) 28, arXiv:1208.6087 [hep-ph].
- [2] S. Bethke, et al., Workshop on precision measurements of α_s , arXiv:1110.0016 [hep-ph];
S. Moch, S. Weinzierl, et al., High precision fundamental constants at the TeV scale, arXiv:1405.4781 [hep-ph];
S. Alekhin, J. Blümlein, S. Moch, DESY 16-051.
- [3] S. Alekhin, J. Blümlein, K. Daum, K. Lipka, S. Moch, *Phys. Lett. B* **720** (2013) 172, arXiv:1212.2355 [hep-ph].
- [4] E. Laenen, S. Riemersma, J. Smith, W.L. van Neerven, *Nucl. Phys. B* **392** (1993) 162;
E. Laenen, S. Riemersma, J. Smith, W.L. van Neerven, *Nucl. Phys. B* **392** (1993) 229.
- [5] S. Riemersma, J. Smith, W.L. van Neerven, *Phys. Lett. B* **347** (1995) 143, arXiv:hep-ph/9411431.
- [6] I. Bierenbaum, J. Blümlein, S. Klein, *Phys. Lett. B* **672** (2009) 401, arXiv:0901.0669 [hep-ph].
- [7] S.I. Alekhin, J. Blümlein, *Phys. Lett. B* **594** (2004) 299, arXiv:hep-ph/0404034.
- [8] M. Buza, Y. Matiounine, J. Smith, R. Migneron, W.L. van Neerven, *Nucl. Phys. B* **472** (1996) 611, arXiv:hep-ph/9601302.
- [9] M. Buza, Y. Matiounine, J. Smith, W.L. van Neerven, *Eur. Phys. J. C* **1** (1998) 301, arXiv:hep-ph/9612398.
- [10] I. Bierenbaum, J. Blümlein, S. Klein, *Nucl. Phys. B* **820** (2009) 417, arXiv:0904.3563 [hep-ph].
- [11] A. Behring, I. Bierenbaum, J. Blümlein, A. De Freitas, S. Klein, F. Wißbrock, *Eur. Phys. J. C* **74** (9) (2014) 3033, arXiv:1403.6356 [hep-ph].
- [12] J. Ablinger, J. Blümlein, S. Klein, C. Schneider, F. Wißbrock, *Nucl. Phys. B* **844** (2011) 26, arXiv:1008.3347 [hep-ph].

- [13] J. Blümlein, A. Hasselhuhn, S. Klein, C. Schneider, Nucl. Phys. B 866 (2013) 196, arXiv:1205.4184 [hep-ph].
- [14] J. Ablinger, A. Behring, J. Blümlein, A. De Freitas, A. Hasselhuhn, A. von Manteuffel, M. Round, C. Schneider, F. Wißbrock, Nucl. Phys. B 886 (2014) 733, arXiv:1406.4654 [hep-ph].
- [15] J. Ablinger, A. Behring, J. Blümlein, A. De Freitas, A. von Manteuffel, C. Schneider, Nucl. Phys. B 890 (2014) 48, arXiv:1409.1135 [hep-ph].
- [16] A. Behring, J. Blümlein, A. De Freitas, A. von Manteuffel, C. Schneider, Nucl. Phys. B 897 (2015) 612, arXiv:1504.08217 [hep-ph].
- [17] A. Behring, J. Blümlein, A. De Freitas, A. Hasselhuhn, A. von Manteuffel, C. Schneider, Phys. Rev. D 92 (11) (2015) 114005, arXiv:1508.01449 [hep-ph].
- [18] J. Blümlein, A. Hasselhuhn, T. Pfoh, Nucl. Phys. B 881 (2014) 1, arXiv:1401.4352 [hep-ph].
- [19] J.A.M. Vermaseren, A. Vogt, S. Moch, Nucl. Phys. B 724 (2005) 3, arXiv:hep-ph/0504242.
- [20] S. Moch, J.A.M. Vermaseren, A. Vogt, Nucl. Phys. B 813 (2009) 220, arXiv:0812.4168 [hep-ph].
- [21] M. Buza, Y. Matiounine, J. Smith, W.L. van Neerven, Nucl. Phys. B 485 (1997) 420, arXiv:hep-ph/9608342; I. Bierenbaum, J. Blümlein, S. Klein, arXiv:0706.2738 [hep-ph]; I. Bierenbaum, J. Blümlein, S. Klein, in preparation.
- [22] M. Buza, W.L. van Neerven, Nucl. Phys. B 500 (1997) 301, arXiv:hep-ph/9702242.
- [23] S.L. Adler, Phys. Rev. 143 (1966) 1144.
- [24] J.D. Bjorken, Phys. Rev. 163 (1967) 1767.
- [25] J.D. Bjorken, Phys. Rev. D 1 (1970) 1376.
- [26] D.J. Gross, C.H. Llewellyn Smith, Nucl. Phys. B 14 (1969) 337.
- [27] J. Blümlein, W.L. van Neerven, Phys. Lett. B 450 (1999) 417, arXiv:hep-ph/9811351.
- [28] W.L. van Neerven, in: A.H. Blin, B. Hiller, M.C. Ruivo, C.A. de Sousa, E. van Beveren (Eds.), Proceedings of the Workshop Hadron Physics: Effective Theories of Low-Energy QCD, Coimbra, Portugal, 1999, in: AIP Conf. Proc., vol. 508, 2000, p. 162, arXiv:hep-ph/9910356; W.L. van Neerven, arXiv:hep-ph/9709469.
- [29] T. Kinoshita, J. Math. Phys. 3 (1962) 650.
- [30] T.D. Lee, M. Nauenberg, Phys. Rev. 133 (1964) B1549.
- [31] J. Blümlein, H. Böttcher, A. Guffanti, Nucl. Phys. B 774 (2007) 182, arXiv:hep-ph/0607200; J. Blümlein, H. Böttcher, A. Guffanti, Nucl. Phys. B, Proc. Suppl. 135 (2004) 152, arXiv:hep-ph/0407089.
- [32] J. Ablinger, J. Blümlein, A. De Freitas, A. Hasselhuhn, C. Schneider, F. Wißbrock, DESY 14-019.
- [33] N. Cabibbo, Phys. Rev. Lett. 10 (1963) 531.
- [34] M. Glück, S. Kretzer, E. Reya, Phys. Lett. B 398 (1997) 381; M. Glück, S. Kretzer, E. Reya, Phys. Lett. B 405 (1997) 392 (Erratum), arXiv:hep-ph/9701364.
- [35] J. Blümlein, A. Hasselhuhn, P. Kovacicova, S. Moch, Phys. Lett. B 700 (2011) 294, arXiv:1104.3449 [hep-ph].
- [36] T. Gottschalk, Phys. Rev. D 23 (1981) 56.
- [37] B. Lampe, E. Reya, Phys. Rep. 332 (2000) 1, arXiv:hep-ph/9810270.
- [38] E.B. Zijlstra, W.L. van Neerven, Nucl. Phys. B 383 (1992) 525; W.L. van Neerven, A. Vogt, Nucl. Phys. B 568 (2000) 263, arXiv:hep-ph/9907472.
- [39] E.G. Floratos, D.A. Ross, C.T. Sachrajda, Nucl. Phys. B 129 (1977) 66; E.G. Floratos, D.A. Ross, C.T. Sachrajda, Nucl. Phys. B 139 (1978) 545 (Erratum); G. Curci, W. Furmanski, R. Petronzio, Nucl. Phys. B 175 (1980) 27.
- [40] J. Kodaira, S. Matsuda, T. Muta, K. Sasaki, T. Uematsu, Phys. Rev. D 20 (1979) 627.
- [41] E.B. Zijlstra, W.L. van Neerven, Nucl. Phys. B 417 (1994) 61; E.B. Zijlstra, W.L. van Neerven, Nucl. Phys. B 426 (1994) 245 (Erratum); E.B. Zijlstra, W.L. van Neerven, Nucl. Phys. B 773 (2007) 105 (Erratum).
- [42] K.A. Olive, et al., Particle Data Group, Chin. Phys. C 38 (2014) 090001, and 2015 update.
- [43] J. Blümlein, H. Böttcher, Nucl. Phys. B 841 (2010) 205, arXiv:1005.3113 [hep-ph].
- [44] J. Blümlein, A. De Freitas, C. Schneider, Nucl. Part. Phys. Proc. 261–262 (2015) 185, arXiv:1411.5669 [hep-ph].
- [45] N. Gray, D.J. Broadhurst, W. Grafe, K. Schilcher, Z. Phys. C 48 (1990) 673; D.J. Broadhurst, N. Gray, K. Schilcher, Z. Phys. C 52 (1991) 111; K.G. Chetyrkin, M. Steinhauser, Nucl. Phys. B 573 (2000) 617, arXiv:hep-ph/9911434; K.G. Chetyrkin, M. Steinhauser, Phys. Rev. Lett. 83 (1999) 4001, arXiv:hep-ph/9907509.
- [46] T. Gehrmann, E. Remiddi, Comput. Phys. Commun. 141 (2001) 296, arXiv:hep-ph/0107173.
- [47] S. Buehler, C. Duhr, Comput. Phys. Commun. 185 (2014) 2703, arXiv:1106.5739 [hep-ph].
- [48] D. Maitre, Comput. Phys. Commun. 174 (2006) 222, <http://dx.doi.org/10.1016/j.cpc.2005.10.008>, arXiv:hep-ph/0507152.

- [49] J. Ablinger, PoS LL 2014 (2014) 019;
 J. Ablinger, A computer algebra toolbox for harmonic sums related to particle physics, Diploma Thesis, J. Kepler University, Linz, 2009, arXiv:1011.1176 [math-ph];
 J. Ablinger, Ph.D. Thesis, J. Kepler University, Linz, 2012, arXiv:1305.0687 [math-ph];
 J. Ablinger, J. Blümlein, C. Schneider, J. Math. Phys. 52 (2011) 102301, arXiv:1105.6063 [math-ph];
 J. Ablinger, J. Blümlein, C. Schneider, J. Math. Phys. 54 (2013) 082301, arXiv:1302.0378 [math-ph];
 J. Ablinger, J. Blümlein, C.G. Raab, C. Schneider, J. Math. Phys. 55 (2014) 112301, arXiv:1407.1822 [hep-th].
- [50] R. Piessens, Angew. Informatik 9 (1973) 399.
- [51] S. Wandzura, F. Wilczek, Phys. Lett. B 72 (1977) 195.
- [52] J. Blümlein, N. Kochelev, Phys. Lett. B 381 (1996) 296, arXiv:hep-ph/9603397.
- [53] J. Blümlein, N. Kochelev, Nucl. Phys. B 498 (1997) 285, arXiv:hep-ph/9612318.
- [54] J. Blümlein, A. Tkabladze, Nucl. Phys. B 553 (1999) 427, arXiv:hep-ph/9812478.
- [55] A. Piccione, G. Ridolfi, Nucl. Phys. B 513 (1998) 301, arXiv:hep-ph/9707478.
- [56] J. Blümlein, B. Geyer, D. Robaschik, Nucl. Phys. B 560 (1999) 283, arXiv:hep-ph/9903520.
- [57] J. Blümlein, D. Robaschik, Nucl. Phys. B 581 (2000) 449, arXiv:hep-ph/0002071.
- [58] B. Geyer, D. Robaschik, J. Eilers, Nucl. Phys. B 704 (2005) 279, arXiv:hep-ph/0407300.
- [59] J. Blümlein, D. Robaschik, Phys. Rev. D 65 (2002) 096002, arXiv:hep-ph/0202077.
- [60] J. Blümlein, D. Robaschik, B. Geyer, Eur. Phys. J. C 61 (2009) 279, arXiv:0812.1899 [hep-ph].
- [61] J. Blümlein, V. Ravindran, W.L. van Neerven, Phys. Rev. D 68 (2003) 114004, arXiv:hep-ph/0304292.
- [62] J.D. Jackson, G.G. Ross, R.G. Roberts, Phys. Lett. B 226 (1989) 159.
- [63] R.G. Roberts, G.G. Ross, Phys. Lett. B 373 (1996) 235, arXiv:hep-ph/9601235.
- [64] H. Burkhardt, W.N. Cottingham, Ann. Phys. 56 (1970) 453.
- [65] V. Ravindran, W.L. van Neerven, Nucl. Phys. B 605 (2001) 517, arXiv:hep-ph/0102280.
- [66] H. Georgi, H.D. Politzer, Phys. Rev. D 14 (1976) 1829.
- [67] A. Zee, F. Wilczek, S.B. Treiman, Phys. Rev. D 10 (1974) 2881.
- [68] D.I. Kazakov, A.V. Kotikov, Nucl. Phys. B 307 (1988) 721;
 D.I. Kazakov, A.V. Kotikov, Nucl. Phys. B 345 (1990) 299 (Erratum);
 D.I. Kazakov, A.V. Kotikov, G. Parente, O.A. Sampayo, J. Sanchez Guillen, Phys. Rev. Lett. 65 (1990) 1535;
 D.I. Kazakov, A.V. Kotikov, G. Parente, O.A. Sampayo, J. Sanchez Guillen, Phys. Rev. Lett. 65 (1990) 2921 (Erratum);
 J. Sanchez Guillen, J. Miramontes, M. Miramontes, G. Parente, O.A. Sampayo, Nucl. Phys. B 353 (1991) 337.
- [69] S. Moch, J.A.M. Vermaseren, Nucl. Phys. B 573 (2000) 853, arXiv:hep-ph/9912355.
- [70] J. Blümlein, A. De Freitas, W.L. van Neerven, S. Klein, Nucl. Phys. B 755 (2006) 272, arXiv:hep-ph/0608024.
- [71] S. Alekhin, J. Blümlein, S. Moch, Phys. Rev. D 89 (5) (2014) 054028, arXiv:1310.3059 [hep-ph], The parameterization is available through <https://lhpdf.hepforge.org/>.
- [72] W. Furmanski, R. Petronzio, Z. Phys. C 11 (1982) 293.
- [73] K.G. Chetyrkin, Talk at loops and legs in quantum field theory, Weimar, <https://indico.desy.de/conferenceOtherViews.py?view=standard&confId=8107>, April 2014.
- [74] P.A. Baikov, K.G. Chetyrkin, J.H. Kühn, J. Rittinger, Phys. Lett. B 714 (2012) 62, arXiv:1206.1288 [hep-ph].
- [75] P.A. Baikov, K.G. Chetyrkin, J.H. Kühn, Phys. Rev. Lett. 104 (2010) 132004, arXiv:1001.3606 [hep-ph].
- [76] A.L. Kataev, V.V. Starshenko, Mod. Phys. Lett. A 10 (1995) 235, arXiv:hep-ph/9502348.
- [77] S.L. Adler, arXiv:0905.2923 [hep-ph].
- [78] S. Moch, M. Rogal, Nucl. Phys. B 782 (2007) 51, arXiv:0704.1740 [hep-ph].
- [79] K. Chetyrkin, private communication.
- [80] D. Mund, B. Maerkisch, M. Deissenroth, J. Krempel, M. Schumann, H. Abele, A. Petoukhov, T. Soldner, Phys. Rev. Lett. 110 (2013) 172502, arXiv:1204.0013 [hep-ex].
- [81] S.G. Gorishnii, S.A. Larin, Phys. Lett. B 172 (1986) 109.
- [82] S.A. Larin, J.A.M. Vermaseren, Phys. Lett. B 259 (1991) 345.
- [83] P.A. Baikov, K.G. Chetyrkin, J.H. Kühn, Nucl. Part. Phys. Proc. 261–262 (2015) 3, arXiv:1501.06739 [hep-ph].
- [84] S.A. Larin, Phys. Lett. B 723 (2013) 348, arXiv:1303.4021 [hep-ph].
- [85] W.A. Bardeen, A.J. Buras, D.W. Duke, T. Muta, Phys. Rev. D 18 (1978) 3998.
- [86] G. Altarelli, R.K. Ellis, G. Martinelli, Nucl. Phys. B 143 (1978) 521;
 G. Altarelli, R.K. Ellis, G. Martinelli, Nucl. Phys. B 146 (1978) 544 (Erratum).
- [87] B. Humpert, W.L. van Neerven, Nucl. Phys. B 184 (1981) 225, [http://dx.doi.org/10.1016/0550-3213\(81\)90217-0](http://dx.doi.org/10.1016/0550-3213(81)90217-0).
- [88] S.A. Larin, F.V. Tkachov, J.A.M. Vermaseren, Phys. Rev. Lett. 66 (1991) 862.
- [89] W.L. van Neerven, E.B. Zijlstra, Phys. Lett. B 272 (1991) 127.

- [90] F.M. Steffens, M.D. Brown, W. Melnitchouk, S. Sanches, *Phys. Rev. C* 86 (2012) 065208, arXiv:1210.4398 [hep-ph].
- [91] D. Boer, M. Diehl, R. Milner, R. Venugopalan, W. Vogelsang, D. Kaplan, H. Montgomery, S. Vigdor, et al., arXiv:1108.1713 [nucl-th];
A. Accardi, J.L. Albacete, M. Anselmino, N. Armesto, E.C. Aschenauer, A. Bacchetta, D. Boer, W. Brooks, et al., arXiv:1212.1701 [nucl-ex].
- [92] D.M. Kaplan, MAP Collaboration, MICE Collaboration, *EPJ Web Conf.* 95 (2015) 03019, arXiv:1412.3487 [physics.acc-ph].
- [93] J.L. Abeleira Fernandez, et al., LHeC Study Group Collaboration, *J. Phys. G* 39 (2012) 075001, arXiv:1206.2913 [physics.acc-ph].
- [94] R. Barbieri, J.A. Mignaco, E. Remiddi, *Nuovo Cimento A* 11 (1972) 824.
- [95] R. Barbieri, J.A. Mignaco, E. Remiddi, *Nuovo Cimento A* 11 (1972) 865.
- [96] M.J.G. Veltman, *Physica* 29 (1963) 186.
- [97] B.A. Kniehl, *Acta Phys. Pol. B* 27 (1996) 3631, arXiv:hep-ph/9607255.
- [98] G.M. Fichtenholz, *Differential- und Integralrechnung*, vol. 3, Deutscher Verlag der Wissenschaften, Berlin, 1964.
- [99] P.J. Rijken, W.L. van Neerven, *Phys. Rev. D* 52 (1995) 149, arXiv:hep-ph/9501373.
- [100] F.J. Yndurain, *The Theory of Quark and Gluon Interactions*, Springer, Berlin, 2006, 474 p.
- [101] J.A.M. Vermaseren, *Comput. Phys. Commun.* 83 (1994) 45.